GEOCAP

Geothermal Capacity Building Program Indonesia - Netherlands

*Date: 31-01-2016*

# WP 3.01
# Resource assessment

**Authors:** S.D.H. Putra, N. Putri, N. Suryantini
**Company/ institute:** ITB

*Document number: GEOCAP-20160131-REP-ITB-WP3.01*

# COOPERATING COMPANIES & UNIVERSITIES

GEOCAP

Geothermal Capacity Building Program Indonesia - Netherlands

*INAGA*

*University of Twente, Faculty ITC*

*IF technology*

*University of Indonesia*

*DNV GL*

*Gadjah Mada University*

*Technical University Bandung*

*Utrecht University, Faculty of Geosciences, Department of Earth Sciences*

*Delft University of Technology, Department of Geotechnology*

*Netherlands Organisation for Applied Scientific Research*

# TABLE OF CONTENTS

Figures

## Tables

# 1 RESOURCE ASSESSMENT OF LOW-MEDIUM ENTHALPY

Situated along the Pacific “ring of fire”, West Java is among the most attractive locations for geothermal energy in Indonesia. It has 21,7% of total geothermal potency associated with volcanic area in Indonesia, which amounts to 6.101 MWe, distributed in 11 regencies. Installed capacity today is 1130 MW, from 5 geothermal plants. However, some challenges are still preventing geothermal energy to look more attractive over other energy resources in Indonesia, especially over fossil fuels.

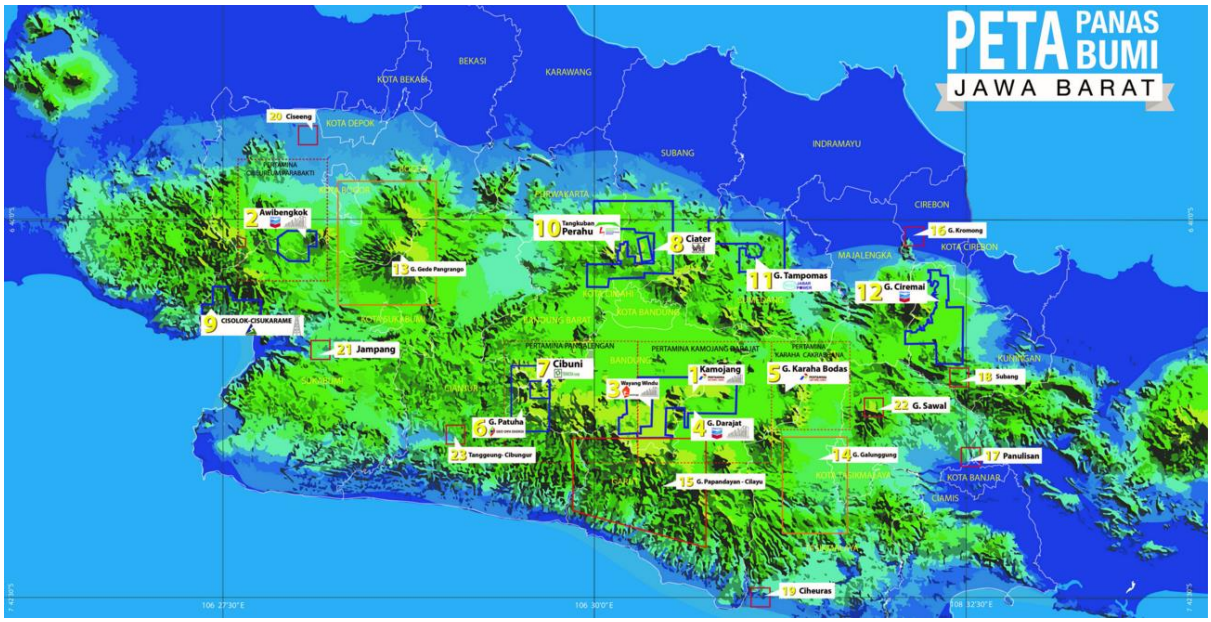


Figure 1 Map of Geothermal Potential in West Java

(Reference: Mineral Resources and Energy Agency of West Java Province)

Even though geothermal is the best option among renewable energy sources to diversify Indonesia’s energy mix and reduce its dependence on fossil fuels, numerous challenges have hindered development, ranging from inadequate incentives to the local people’s concern. The reason for the concern is mostly revolving around the environmental issue which should be properly understood as a feedback for the government (both local and central), developers, and other institutions (e.g. academic or research institution and NGO) to talk more to them and share them more knowledge on geothermal energy therefore they can see the benefits of one of sustainable energy resources existing in their living area, while at the same time assuring appropriate responsibility to protect the environment as a commitment for all.

## 1.1 TYPES OF GEOTHERMAL ENERGY SYSTEM

The conventional type of geothermal energy is the most popular type in Indonesia, which is found in volcanic area where the reservoir rock is close to the surface and provides geothermal fluid with high temperature (>225°C) to power the conventional power plants and generate electricity. The reservoir volcanic rock contains water and/or steam. If the reservoir only contains steam, it is called dry-steam geothermal field which is very rare to be discovered. In Indonesia, there are only two dry-steam geothermal fields have been explored from which have been generating electricity for almost 30 years, i.e. Kamojang and Darajat. While others are water (liquid) and steam (vapour) mixture geothermal fields, or commonly called as two-phase geothermal field. This geothermal energy system is classified as volcanic hydrothermal reservoir system.

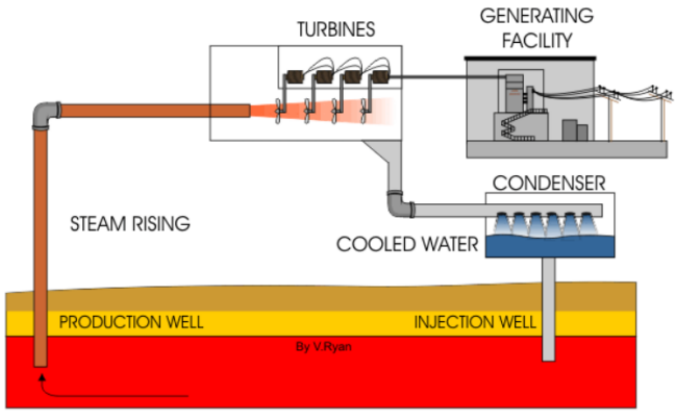


Figure 2 Schematic of dry-steam geothermal power plants

Since the steam from dry-steam geothermal steam is pure steam with very high dryness, therefore it can directly drive a turbine (**Fig.2**). If water and steam mixture produced from reservoir, it is needed an additional process (**Fig.3**), which involves the separation of steam from its liquid body (in more detail, the liquid is vaporizing into steam when entering the "flash tanks" or separator by lowering the fluid pressure to make it vaporize), hence only steam can directly drives a turbine. The waste liquid or commonly called as the waste brine with temperature after separation is still quite high (≈170°C) is re-injected into the reservoir to maintain the sustainability of reservoir.

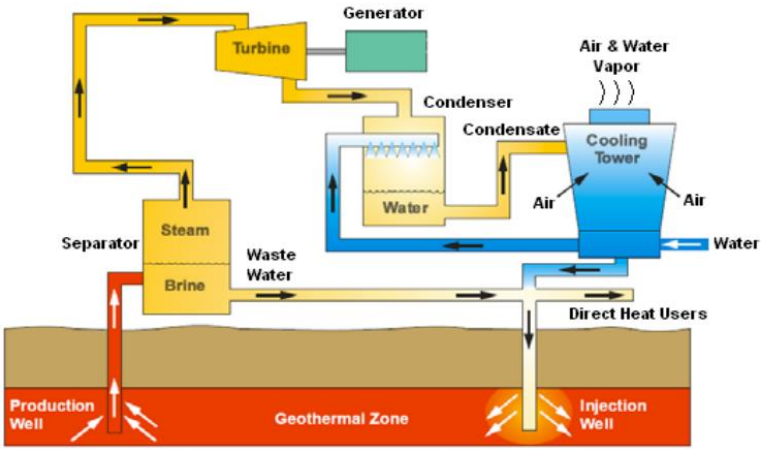


Figure 3 Schematic of flash geothermal power plants

The other main characteristic of volcanic hydrothermal geothermal system is the occurrence of surface manifestation. These manifestations are the surface features that first tell there are geothermal potentials below the surface. They occur on the surface when fluids leak to the surface along faults and fissures through permeable rock. Depending of the temperature reservoir and discharge rate the manifestation can form as hot springs, boiling springs, geysers, fumarole, mud pool, phreatic explosion craters, zones of acid alteration, etc. Consequently, the early prediction of reservoir temperature and composition is done by measuring the manifestation temperature and further studied by hydro-geochemical techniques.

Beside volcanic hydrothermal geothermal system, to date, it has been discovered alternative type of geothermal energy resource which does not require hydrothermal naturally exists from below the surface. But since we still need fluid as heat transfer medium to drive a turbine, as long as it can be discovered potential heat below the surface therefore the cold water can be injected through the injection well that reach the hot bedrock. Then the cold water injected is expected to be heated up conductively by the hot bedrock into some degrees higher before being produced from the producing well to generate electricity or for other purposes. This alternative type of geothermal resource is known as Enhanced Geothermal System (EGS).

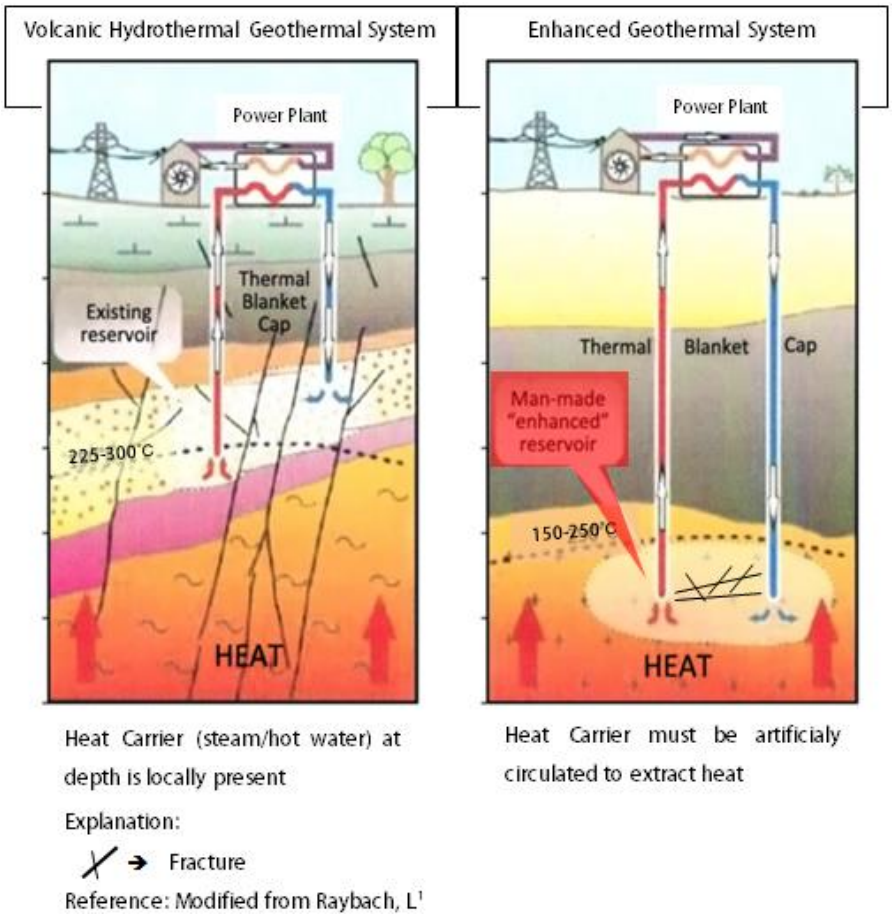


Figure 4 Diagram showing the difference between Volcanic Hydrothermal Geothermal System and Enhanced Geothermal System

The main difference between EGS and volcanic hydrothermal reservoir system, apart from the presence of natural water beneath the surface, is the rock permeability. In EGS, a reservoir is artificially created to make it more permeable to flow the fluid. The flow rate or the productivity or (the rock permeability) can be improved by pumping high pressure water down the wells to open the pathways or fractures in the reservoir. This technique is known as hydraulic-thermal fracture stimulation. While in volcanic hydrothermal reservoir system, the permeability has been created naturally in the reservoir rock due to the plate tectonic collision or divergence which triggers faults which commonly provides fractures or high permeable pathways in the reservoir rock. However, in some hydrothermal systems the permeability of the reservoir may be too low to enable the water to flow at a sufficient rate for electricity generation. Therefore, in an effort to enhance the productivity, the hydraulic-thermal fracture stimulation is sometimes conducted. The stimulation in volcanic hydrothermal system is conducted to open the pathways to the greater fracture network within the high temperature reservoir, therefore the underground fluid from the reservoir can flow freely to the well through the pathways which have been created by hydraulic-thermal stimulation. As long as a well can reach high temperature body in the reservoir, although

without evidence of the fluid yet, the stimulation is always necessary to try, therefore not much money is wasted for having unproductive well.

Other alternative of geothermal energy resource is Hot Sedimentary Aquifer (HSA). Quite similar to that in EGS, which is not associated with volcanic area, but different from EGS in a way of the presence of natural water. HSA tends to develop relatively good porosity in its aquifer, hence more chance for the fluid to fill in. The porous aquifer containing water is heated by either crustal heat flow or proximate hot rocks. But since it is not associated with volcanic magmatic area, the temperature is not as high as in hydrothermal volcanic geothermal system at the same depth. If necessary, fracturing may still be conducted to enhance water flow between wells.

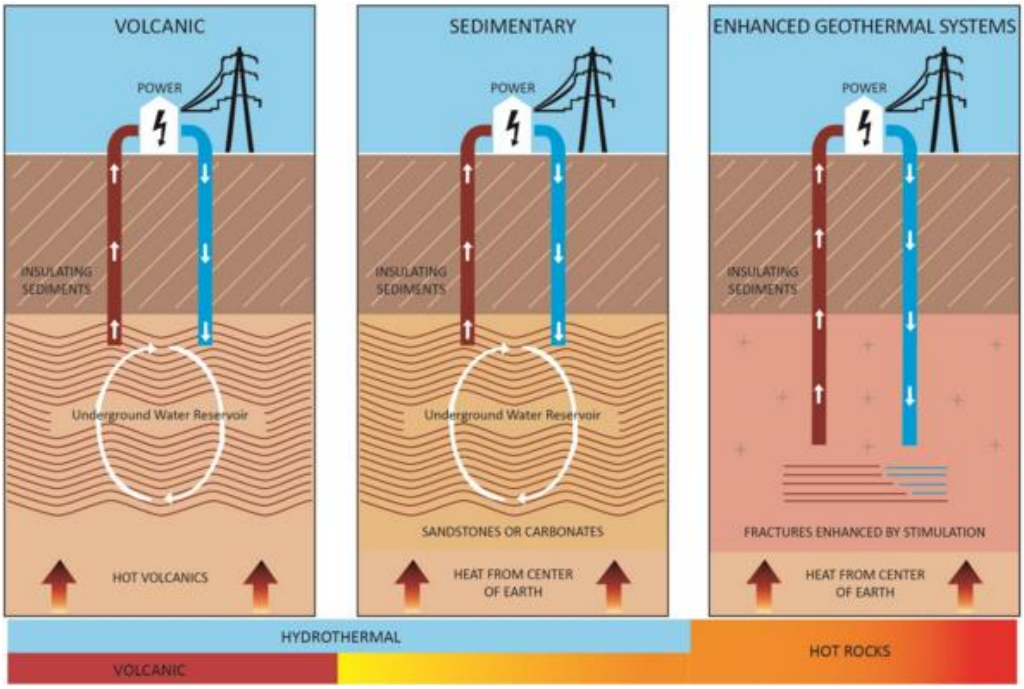


Figure 5 Diagram showing the difference between Volcanic Hydrothermal Geothermal System, Hot Sedimentary Aquifer and Enhanced Geothermal System[2]

The name of Hot Sedimentary Aquifer refers to the sedimentary basin which hosts the aquifer. In West Java, sedimentary basin is spread both off the shore and on the shore of Java (**Fig. 6**), known as Northwest Java Basin, which has been explored for petroleum prospectivity. Although geothermal and petroleum exploration differ in the resource they are looking for – high-temperature water versus hydrocarbons, most data collected for petroleum exploration can and have been used for geothermal exploration (Deming 1989). According to old data of oil and gas well logging collected in Northwest Java Basin, the temperature gradient in some wells show indications of convective heat transfer, which may be identified as the presence of fluid in the porous rock to some extent. However, the data is relatively sparse which makes it more challenging to analyse.

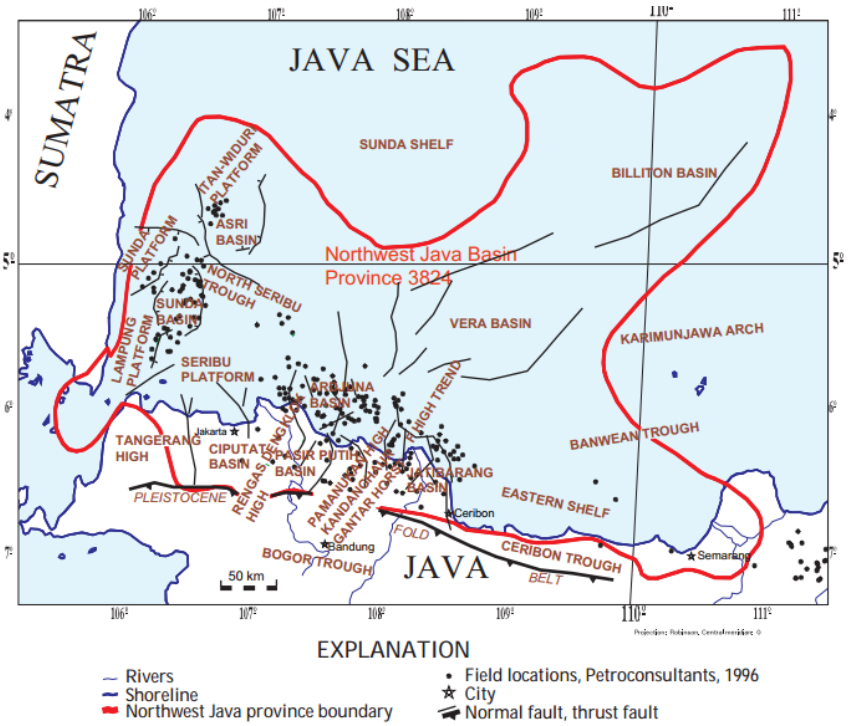


Figure 6 Northwest Java Sedimentary Basin Map

## 1.2 GEOTHERMAL TEMPERATURE RESOURCE CLASSIFICATION

Temperature is a fundamental measure to identify the quality of the geothermal resources. They are defined as low to high based on the temperature achieved at a certain depth. Mostly the classification of geothermal temperature falls into three categories according to the reservoir fluid temperature, i.e. high, intermediate (medium or moderate), and low (**Fig.7**).

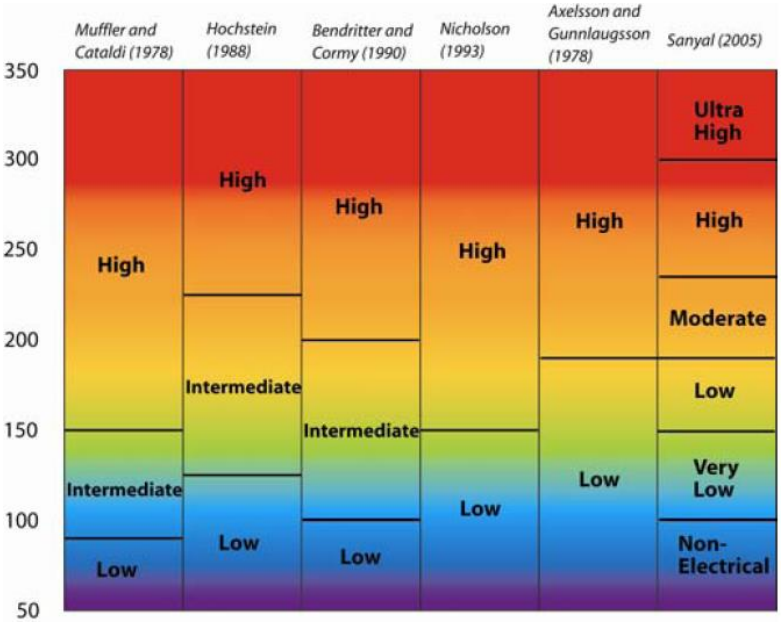


Figure 7 Geothermal Resource Temperature Classification

Note on "Low-Medium Temperature Geothermal Resource"

Based on above classification, the range of temperature of each class varies very widely, to make it less complicated, for this study we learn to assess any geothermal resource with temperature of maximum 200°C, as it is considered to be relatively too low for electricity generation using conventional power plant technology.

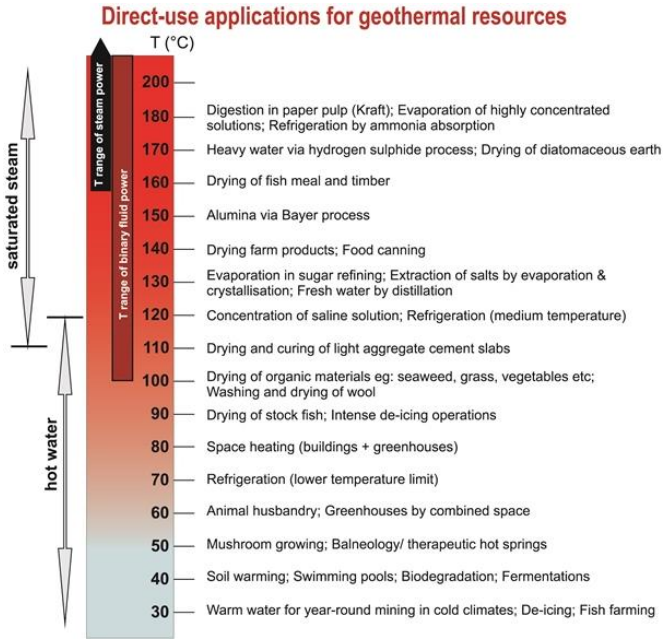


Figure 8 Applications for geothermal resources based on temperature

# 2 GEOTHERMAL POTENTIAL IN WEST JAVA

As previously mentioned, West Java Province has 21.7% of total geothermal potential in Indonesia. 5 geothermal power plants from high enthalpy (high temperature) reservoir have been generating 1134 MW (**Figure 1**).

Herewith the list of geothermal power plants in West Java Province:

1. Kamojang (200 Mwe, Developer : PT Pertamina Geothermal Energy (PGE))
2. Awibengkok (377 Mwe, Developer : PT Chevron Geothermal Salak)
3. Wayang Windu (227 Mwe, Developer : Star Energy Geothermal Wayang Windu and PGE)
4. Darajat (270 Mwe, Developer : PT Chevron Geothermal Indonesia and PGE)
5. Patuha (60 Mwe, Developer : PT Geo Dipa Energi)

Kamojang and Darajat geothermal fields are dry-steam fields, therefore there is no brine wasted or reinjected into reservoir, however there is still possible waste heat to be utilized for direct use. The reinjection fluid is only from the condensate of the steam cooling in condenser. While, Awibengkok, Wayang Windu, and Patuha, are two-phase fields, in which the reservoir produce both liquid and steam. The details of brine flow rate and temperature are given in **paragraph 2.3**. While in **paragraph 2.1** and **paragraph 2.2**, we discuss the potential Hot Springs and Hot Sedimentary Aquifer, respectively.

Other geothermal prospects can be seen in **Figure 10**, where there are 43 geothermal prospect areas distributed in 11 regencies. The detail prospects and their manifestations are listed from **Figure 11** to **24**.


Figure 9 Geothermal resource map of West Java Province

Reference: Mineral Resources and Energy Agency of West Java Province

Geothermal Potential Area in West Java Province (number as shown in map in previous page)

| | | |
|---|---|---|
| 1. Kamojang<br>Potency: 300 MW<br>Field Status: Installed capacity of 200 MWe<br>Developer: PT. Pertamina Geothermal Energy (PGE)<br>Manifestation Area: Kamojang, Masigit-Guntur | 6.Patuha<br>Potency:163 MW<br>Field Status: Installed capacity of 60MW<br>Developer: PT Geo Dipa Energi<br>Manifestation Area: Gunung Urug, Gunung Patuha, Kawah Ciwidey | 11.Tampomas<br>Potency:34 MW<br>Field Status: Prepare for expl.drilling<br>Developer: PT. Wika Jabar Power<br>Manifestation Area: Gn.Tampomas |
| 2. Awibengkok<br>Potency: 495 MW<br>Field Status: Installed capacity of 377 MWe<br>Developer: PT. Chevron Geothermal Salak<br>Manifestation Area: Kawah Ratu, Kiara Beres, Awibengkok, Cibeureum, Cikuluwung | 7.Cibuni<br>Potency: 45 MW<br>Field Status: Exploration drilling<br>Developer: PT. Yala Tekno Geothermal<br>Manifestation Area: Kawah Cibuni | 12.Ciremai<br>Potency:150 MW<br>Field Status: Permit not yet issued<br>Developer: PT Jasa Day Chevron<br>Manifestation Area: Sangkanhurip, Ciniru, Pejambon, Cibingbin,Liangpanas |
| 3. Wayang Windu<br>Potency: 440 MW<br>Field Status: Installed capacity of 227 MWe<br>Developer: JOC PT.PGE and Star Energy Geothermal Wayang Windu<br>Manifestation Area: Gunung Wayang Windu | 8.Ciater<br>Potency: 6 MW<br>Field Status: Exploration Survey<br>Developer: PT. Wahana Sembada Sakti<br>Manifestation Area: Ciater | 13.Gede Pangrango<br>14.Galunggung (Gn. Galunggung)<br>15.Papandayan (Cilayu, Ciarinem, Gn. Papandayan)<br>16.Gunung Kromong (Banyupanas,Goa Macan,Cipanas, Simeut,Gn.Kuda)<br>17.Panulisan 18.Subang<br>19.Ciheuras 20.Ciseeng 21.Jampang<br>22.Sawal (Gn. Sawal , Cipanas-Ciawi)<br>23.Tanggeng-Cibungur |
| 4. Darajat<br>Potency: 400 MW<br>Field Status: Installed capacity of 270 MWe<br>Developer: JOC PT PGE and PT Chevron Geothermal Indonesia<br>Manifestation Area: Darajat | 9.Cisolok-Cisukarame<br>Potency: 58 MW<br>Field Status: Exploration drilling<br>Developer: PT. Jabar Rekind Geothermal<br>Manifestation Area: Cisolok, Cisukarame | |
| 5. Karaha Bodas<br>Potency: 214 MW<br>Field Status: EPCC(Engineering,Procurement,Construction,Commissioning)<br>Developer: PT Pertamina Geothermal Energy<br>Manifestation Area:Telaga Bodas, Gunung Karaha | 10.Tangkuban Perahu<br>Potency: 79 MW<br>Field Status: Exploration drilling<br>Developer: PT Tangkuban Perhau Geothermal Power<br>Manifestation Area: Maribaya, Tangkuban Parahu, Sagalaherang, Saguling-Cimanggu | |

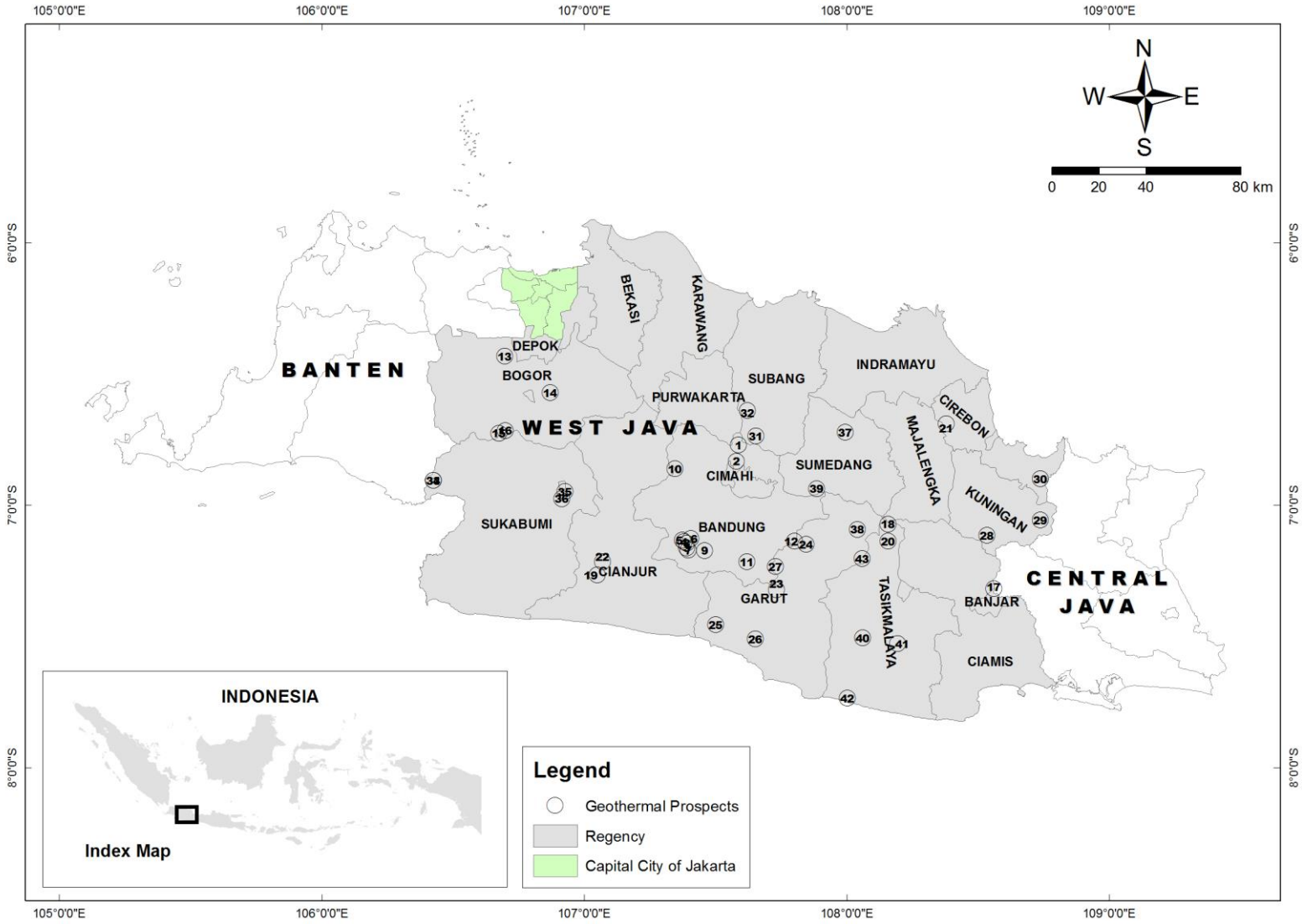


Figure 10 Geothermal prospect map of West Java Province

| NAME OF PROSPECT | TYPE OF SURFACE MANIFESTATION | NEARBY POWER PLANT | LOCATION | SURFACE TEMPERATURE (°C) | GEOTHERMOMETER TEMPERATURE (°C) | TYPE OF FLUID MEASURED | FLOW RATE (l/s) | CHEMICAL CONTENT |
|---|---|---|---|---|---|---|---|---|
| TANGKUBAN PARAHU (1) | Active Silica Sinter | - | Kecamatan Lembang, Cisarua, dan Parompong | | 240-250 | | | |
| | Hot Springs | | | | | | | |
| | - Ciracas | | | 41.6-46 | | Liquid | 0.2 | pH: 5.74-6.66, HCO3 type |
| | - Batu Gede | | | 42.1-45.5 | | Liquid | 0.2-1 | pH: 5.66-6.43, Cl-HCO3 type |
| | - Kawah Domas | | | 85.5 -91.1 | | Liquid | 0.3-2 | pH: 1.27-2.45, SO4 type, H2S |
| | - Kancah | | | 31.1-34.5 | | Liquid | 3.3-5.1 | pH: 2.86- 3.43, SO4 type, H2S |
| | - Cimanggu | | | 34.1-35.2 | | Liquid | 2.3-2.85 | pH: 6.05-7.01, HCO3 type |
| | Mud Pools | | | | | Liquid | | |
| | Rock Alteration | | | | | | | |
| | Solfatara | | | | | | | H2S |
| | - Kawah Ratu | | | 90-100 | | Vapor | | |
| | - Kawah Baru | | | 172 | | Vapor | | |
| | Steaming Ground | | | | | Vapor | | |
| | Volcanic Crater | | | | | | | |
| Maribaya (2) | Hot Springs | - | Desa Lengansari, | 45.1-46.6 | 250 | Liquid | 0.23-1.1 | pH: 5.46-6.38, HCO3 type |
| | Sinter Travertine | | | | | | | |
| Patuha (3) | Volcanic Crater | GEO DIPA | Kecamatan Ciwidey, Rancabali, dan Pasirjambu | | >240 (up to 270) | | | |
| | Hot Springs | | | 35-83 | | Liquid | 2-15 | H2S |
| | Fumarol | | | 93 | | Vapor | | H2S |
| | Solfatara | | | | | Vapor | | |
| | Cool Mudpool | | | | | Liquid | | |
| | Surface alteration | | | | | | | |
| | Silica Sinter | | | | | | | |
| Cimanggu (4) | Hot Springs with sulfur deposits and iron oxide | GEO DIPA | Kecamatan Ciwidey | 40-55 | 240 | Liquid | 7.82-15.87 | H2S |
| | Travertine | | | | | | | |
| Rancawalini (5) | Ebulliant hotsprings (CO2) with sulfur deposit | GEO DIPA | Kecamatan Ciwidey | 40-55 | 240 | Liquid | 7.17-15.87 | CO2 |
| | Iron Oxide and carbonate sinter | | | | | | | |
| Barutunggul (6) | Hot Springs with iron oxide and travertine | GEO DIPA | Kecamatan Pasirjambu | 41 | 270 | Liquid | | |
| Kawah Putih (7) | Acid warm springs | GEO DIPA | Kecamatan Pasirjambu | | 240 | Liquid | | |
| | Mud Pools | | | | | Liquid | | |
| | Solfatara | | | 90-95 | | Vapor | | H2S |
| | Steaming Ground | | | | | Vapor | | |
| Cibuni Crater (8) | Steaming Ground | GEO DIPA | Kecamatan Rancabali | | 240 | Vapor | | |
| | Fumarol | | | 90-95 | | Vapor | | |
| | Solfatara | | | | | Vapor | | |
| | Mud Pools | | | | | Liquid | | |
| | Hot springs | | | 85-90 | | Liquid | >3 | Acidic Sulphate Water |
| | Extensive surface alteration rock | | | | | | | |
| Ciwidey (9) | Fumarol | GEO DIPA | Kampung Cibogo/Cobra Desa Alam Endah Kecamatan | 90-95 | 240 | Vapor | | |
| | Solfatara | | | | | Vapor | | |
| | Mud Pools | | | | | Liquid | | |
| | Hot Springs | | | 70-90 | | Liquid | >4 | Acidic Sulphate Water |
| | Surface Alteration Rock | | | | | | | |
| Saguling Rajamandala (10) | Hot springs | | Desa Saguling Kecamatan Cipatat | 75.6 | 120-135 | Liquid | | |

Figure 11 Geothermal manifestation area in Bandung Regency (1/2)

| NAME OF PROSPECT | TYPE OF SURFACE MANIFESTATION | NEARBY POWER PLANT | LOCATION | SURFACE TEMPERATURE (°C) | GEOTHERMOMETER TEMPERATURE (°C) | TYPE OF FLUID MEASURED | FLOW RATE (l/s) | CHEMICAL CONTENT |
|---|---|---|---|---|---|---|---|---|
| Wayang Windu (11) | Hot and nearly boiling springs | STAR ENERGY WAYANG WINDU | Kecamatan Pangalengan | 39-66 | 250-270 | Liquid | 15 | |
| | Steaming Ground | | | | | Vapor | | |
| | Fumarol | | | 93 | | Vapor | | |
| | Solfatara | | | | | Vapor | | |
| | Geyser | | | | | Liquid | | |
| | Surface Alteration | | | | | | | |
| | Silica Sinter | | | | | | | |
| | Fosil Hydrothermal System with Sulfur Deposit | | | | | | | |
| Kamojang (12) | Hot Springs | PGE KAMOJANG | Kecamatan Ibun dan Paseh, Kabupaten Bandung | | 245 | | | |
| | - Kawah Kamojang | | | 90-93 | | Liquid | 2 | Sulphate Waters with pH 2.7 |
| | - Kawah Hujan | | | 94 | | Liquid | 2 | Acidic Sulphate Water |
| | - Citepus Hotspring | | | 55-60 | | Liquid | 2 | Bicarbonate Water |
| | Fumarol | | | | | | | |
| | - Kawah Hujan | | Kecamatan Leles dan Samarang, Kabupaten Garut | 94 | | Vapor | | |
| | Mud Pools | | | 93-95 | | | | |
| | - dry mud pool and small mud volcano in Kawah Sa | | | 90 | | Liquid | | |
| | - mud pool in Kawah Berecek | | | 93-94 | | Liquid | | very acidic fluids |
| | - mud pools, small mud volcano, and a mud crack c | | | 93-95 | | Liquid | | acidic fluids with pH 3.5-4 |
| | Vulcanic Crater | | | | | | | |
| | Surface Alteration | | | | | | | |

Figure 12 Geothermal manifestation area in Bandung Regency (2/2)

| NAME OF PROSPECT | TYPE OF SURFACE MANIFESTATION | NEARBY POWER PLANT | LOCATION | SURFACE TEMPERATURE (°C) | GEOTHERMOMETER TEMPERATURE (°C) | TYPE OF FLUID MEASURED | FLOW RATE (l/s) | CHEMICAL CONTENT |
|---|---|---|---|---|---|---|---|---|
| Ciseeng (13) | Warm Springs with Travertine Deposit | - | Kampung Ciseeng Desa Bojong Indah Kecamatan Parung | 44.3 | | Liquid | 0.5 | |
| G. Pancar-Sanggabuana (14) | Hot Springs : | - | Kampung Cimandala, Desa Karang Tengah, Kecamatan Babakan Madang | | Mod-high H | | | |
| | 1 | | | 54.4 | | Liquid | | |
| | 2 | | | 52.9 | | Liquid | | |
| | 3 | | | 59.1 | | Liquid | | |
| | 4 | | | 53.1 | | Liquid | | |
| | 5 | | | 65.2 | | Liquid | | |
| | 6 | | | 67.2 | | Liquid | | |
| | Sinter Travertine | | | | | | | |

Figure 13 Geothermal manifestation area in Bogor Regency (1/2)

| NAME OF PROSPECT | TYPE OF SURFACE MANIFESTATION | NEARBY POWER PLANT | LOCATION | SURFACE TEMPERATURE (°C) | GEOTHERMOMETER TEMPERATURE (°C) | TYPE OF FLUID MEASURED | FLOW RATE (l/s) | CHEMICAL CONTENT |
|---|---|---|---|---|---|---|---|---|
| Awibengkok-G. Salak (15) | Hot Springs | CHEVRON G. SALAK | Kecamatan Pamijahan, Kab. Bogor and Kecamatan Kabandungan & Kalapanunggal, Kab.Sukabumi | | 245-325 | | | |
| | - Cibodas | | | 65.7 | | Liquid | 0.13 | pH: 6.5 |
| | - Ciherang 1 | | | 39.3 | | Liquid | 0.03 | pH: 6.8 |
| | - Ciherang 2 | | | 35.3 | | Liquid | 0.17 | pH: 6.5 |
| | - Awi Barat | | | 63.7 | | Liquid | | pH: 7.1 |
| | - Ciseupan | | | 42.6 | | Liquid | | pH: 6.5 |
| | - Cisaketi 1 | | | 40 | | Liquid | | |
| | - Cisaketi 2 | | | 39 | | Liquid | | |
| | - Cisaketi 3 | | | 42.1 | | Liquid | 0.33 | |
| | - Cipanas Karang | | | 71.2 | | Liquid | 0.07 | pH: 6.5 |
| | - Muhinin | | | 40 | | Liquid | 0.03 | pH: 6.5 |
| | - Sarimaya | | | 61.2 | | Liquid | 0.08 | pH: 6.5 |
| | - Cianten | | | 33 | | Liquid | | pH: 5.8 |
| | - Cipanas Cikuluwung | | | 47.2 | | Liquid | 0.15 | pH: 7 |
| | - Cihideung | | | 46 | | Liquid | 0.18 | pH: 6.5 |
| | Hot Pools | | | | | | | |
| | - Cipamatutan 1 | | | 86 | | Liquid | | |
| | - Cipamatutan 2 | | | 98 | | Liquid | | pH: 3.9 |
| | Fumaroles | | | | | | | |
| | - Getih (Cibeureum) 1 | | | 96.1 | | Vapor | | |
| | - Getih (Cibeureum) 2 | | | 98 | | Vapor | | |
| | - Parabakti 1 | | | 104 | | Vapor | | |
| | - Parabakti 2 | | | 94.7 | | Vapor | | |
| | - Cipamatutan | | | 95 | | Vapor | | |
| Kawah Ratu-G. Salak (16) | Hot Springs : | CHEVRON G. SALAK | Kawah Ratu G. Salak Kampung Ciparay Desa Gunung Sari Kecamatan Pamijahan | | 225-325 | | | |
| | 1 | | | 45.9 | | Liquid | 2 | pH : 6.07 |
| | 2 | | | 40.3 | | Liquid | 1 | pH : 6.46 |
| | Fumarol | | | 126 | | Vapor | | |
| | Mud Pools | | | | | Liquid | | |
| | Vulcanic Crater | | | | | | | |
| | Surface Alteration | | | | | | | |

Figure 14 Geothermal manifestation area in Bogor Regency (2/2)

| NAME OF PROSPECT | TYPE OF SURFACE MANIFESTATION | NEARBY POWER PLANT | LOCATION | SURFACE TEMPERATURE (°C) | GEOTHERMOMETER TEMPERATURE (°C) | TYPE OF FLUID MEASURED | FLOW RATE (l/s) | CHEMICAL CONTENT |
|---|---|---|---|---|---|---|---|---|
| Panulisan (17) | Warm Springs with Travertine Deposit and iron oxide | - | Kecamatan Banjar | 44-52 | 120 | Liquid | 2 | pH: neutral |
| | Altered Ground | | | | | | | |
| | Fossil of Solfatara | | | | | Vapor | | |
| G. Sawal (18) | Warm Spring | - | Kampung Cikoranji, Desa Tanjungkerta, | 37.7 | | Liquid | | |

Figure 15 Geothermal manifestation area in Ciamis Regency

| NAME OF PROSPECT | TYPE OF SURFACE MANIFESTATION | NEARBY POWER PLANT | LOCATION | SURFACE TEMPERATURE (°C) | GEOTHERMOMETER TEMPERATURE (°C) | TYPE OF FLUID MEASURED | FLOW RATE (l/s) | CHEMICAL CONTENT |
|---|---|---|---|---|---|---|---|---|
| Tanggeung-Cibungur-Cibuni (19) | Hot Spring 1 | GEO DIPA | Kampung Sirnagalih, Desa Margaluyu Kecamatan Tanggeung | 70.5 | 72 | Liquid | 2 | pH : 6.3 |
| | Hot Spring 2 | | | 69.1 | | Liquid | - | pH : 6.26 |
| Cipanas-Pacet (20) | Warm Springs | GEO DIPA | Desa Cipanas | 40 | 103-197 | Liquid | 0.8 | - |

Figure 16 Geothermal manifestation area in Cianjur Regency

| NAME OF PROSPECT | TYPE OF SURFACE MANIFESTATION | NEARBY POWER PLANT | LOCATION | SURFACE TEMPERATURE (°C) | GEOTHERMOMETER TEMPERATURE (°C) | TYPE OF FLUID MEASURED | FLOW RATE (l/s) | CHEMICAL CONTENT | HEAT IN PLACE |
|---|---|---|---|---|---|---|---|---|---|
| G. Kromong (21) | Mud Pools | - | Kampung Curug/ Banyu Panas Desa Palimanan Barat | | Low H | Liquid | | | |
| | Hot Pools | | | | | Liquid | | | |
| | Hot Springs | | | 57 | | Liquid | 4 | pH : 6.25 | 377.55 kW |
| | Silica Sinter | | | | | | | | |
| | Travertine | | | | | | | | |
| | Altered Ground | | | | | | | | |

Figure 17 Geothermal manifestation area in Cirebon Regency

| NAME OF PROSPECT | TYPE OF SURFACE MANIFESTATION | NEARBY POWER PLANT | LOCATION | SURFACE TEMPERATURE (°C) | GEOTHERMOMETER TEMPERATURE (°C) | TYPE OF FLUID MEASURED | FLOW RATE (l/s) | CHEMICAL CONTENT |
|---|---|---|---|---|---|---|---|---|
| Talaga Bodas (22) | Hot Springs | - | Desa Cicapar, Kecamatan Wanaraja | 68.1 | 220 | Liquid | 7 | pH: 6.39 |
| | Fumarol | | | | | Vapor | | |
| | Solfatara | | | | | Vapor | | |
| | Sulfur Deposit around Vent | | | | | | | |
| | Weak Ebullient | | | | | | | |
| | Hydrothermal Alteration | | | | | | | |
| Papandayan (23) | Vulcanic Crater | - | Kecamatan Cisurupan, Kab. Garut & Kecamatan Pangalengan Kab. Bandung | | 230 | | | |
| | Fumaroles | | | | | | | |
| | - Kawah Mas | | | 260 | | Vapor | | Sulphur |
| | - Kawah Manuk | | | 105 | | Vapor | | Sulphur |
| | - Kawah Nangklak | | | 92 | | Vapor | | Sulphur |
| | - Kawah Welirang | | | 92 | | Vapor | | Sulphur |
| | Hot Ground | | | | | | | |
| | Altered Ground | | | | | | | |
| | Hot Springs | | | | | | | |
| | - Kawah Mas | | | 79 | | Liquid | 0.17 | pH: 1.8, H2S |
| | - Kawah Manuk | | | 65 | | Liquid | 0.17 | pH: 1.7, H2S |
| | - Kawah Nangklak | | | 91 | | Liquid | | pH: 2.7, H2S |
| | - Cibeureum Leutik | | | 32 | | Liquid | 0.25 | pH: 2.7, H2S |
| | Crater Lake (Kawah Baru) | | | 26 | | Liquid | | pH: 2.6, H2S |
| | Mud Pools | | | | | | | |
| | - Kawah Manuk | | | 89 | | Liquid | | pH: 1.1, H2S |
| Cipanas-Tarogong (G. Masigit-Guntur) (24) | Hot Springs | - | Kampung Cipanas, Desa Langeunsari, Kecamatan Tarogong Kaler | 45 | 206 | Liquid | 2 | pH: 6.37, Sulphate 50.5% |

Figure 18 Geothermal manifestation area in Garut Regency (1/2)

| NAME OF PROSPECT | TYPE OF SURFACE MANIFESTATION | NEARBY POWER PLANT | LOCATION | SURFACE TEMPERATURE (°C) | GEOTHERMOMETER TEMPERATURE (°C) | TYPE OF FLUID MEASURED | FLOW RATE (l/s) | CHEMICAL CONTENT |
|---|---|---|---|---|---|---|---|---|
| Cilayu (25) | Hot Springs | - | Kampung Cipanas, Desa Sukajaya, Kecamatan Cisewu | 61 | 168 | Liquid | 1 | pH: 6.26, Cl |
| | Hydrothermal Alteration | | | | | | | |
| | Travertine and iron oxide around the s | | | | | | | |
| Ciarinem (26) | Hot Springs | - | Kampung Cipanas, Desa Sukamulya, Kecamatan | 52 | 120 | Liquid | | pH: 6.17 |
| | Hydrothermal Alteration | | | | | | | |
| Kawah Darajat (27) | Vulcanic Crater | CHEVRON DARAJAT | Kecamatan Pasirwangi | | 245 | | | |
| | Fumaroles | | | 118 | | Vapor | | |
| | Hot Ground | | | | | | | |
| | Altered Ground | | | | | | | |
| | Hot Springs | | | | | | | |
| | - Cibeureum 1 | | | 51 | | Liquid | | |
| | - Cibeureum 2 | | | 48 | | Liquid | | |
| | - Toblong 1 | | | 54 | | Liquid | | |
| | - Toblong 2 | | | 56 | | Liquid | | |
| | - Warm seep at Toblong | | | | | Liquid | | pH: 3, SO4 type |
| | - Golangsing | | | 29 | | Liquid | | pH: 4-5, SO4 type |
| | Boiling Pool | | | | | Liquid | | |
| | Mud Pools | | | | | Liquid | | |

Figure 19 Geothermal manifestation area in Garut Regency (2/2)

| NAME OF PROSPECT | TYPE OF SURFACE MANIFESTATION | NEARBY POWER PLANT | LOCATION | SURFACE TEMPERATURE (°C) | GEOTHERMOMETER TEMPERATURE (°C) | TYPE OF FLUID MEASURED | FLOW RATE (l/s) | CHEMICAL CONTENT | HEAT IN PLACE |
|---|---|---|---|---|---|---|---|---|---|
| Subang (Cikadu) (28) | Hot Springs | - | Kampung Cikadu, Desa Subang, Kecamatan Subang | | 90 | Liquid | | | 506.86 KW |
| | - Hot Spring Subang 1 | | | 60.5 | | Liquid | 2 | pH: 6.32, Cl type | |
| | - Hot Spring Subang 2 | | | 60.8 | | Liquid | 0.5 | pH: 6.15, Cl type | |
| | - Hot Spring Subang 3 | | | 60.9 | | Liquid | 0.5 | pH: 6.04, Cl type | |
| | - Hot SpringsSubang 4 | | | 60.7 | | Liquid | 0.5 | pH: 5.98, Cl type | |
| Cibingin (29) | Hot Springs | - | Kampung Cipanas, Desa Ciangir, Kecamatan Cibingbin | 54.2 | 132.5 | Liquid | 3 | pH: 6.17, Cl type | 261.95 KW |
| G. Ciremai-Sangkahurip (30) | Hot Springs | - | | 48 | | Liquid | | | |

Figure 20 Geothermal manifestation area in Kuningan Regency

| NAME OF PROSPECT | TYPE OF SURFACE MANIFESTATION | NEARBY POWER PLANT | LOCATION | SURFACE TEMPERATURE (°C) | GEOTHERMOMETER TEMPERATURE (°C) | TYPE OF FLUID MEASURED | FLOW RATE (l/s) | CHEMICAL CONTENT |
|---|---|---|---|---|---|---|---|---|
| Ciater (31) | Hot Springs with silica deposits, iron | | Kecamatan Subang | 44-46.9 | 200-210 | Liquid | 2 – 15 | pH: 1.8-2.8, Cl-H2S type |
| Sagalaherang (Batu Kapur) (32) | Hot Springs | - | Desa Curug Agung, Kecamatan Sagalaherang | 39.4-40.1 | 190-200 | Liquid | 2.2 – 3.9 | pH: 5.49-6.2, HCO3 type |
| | Travertine, iron oxide around the | | | | | | | |

Figure 21 Geothermal manifestation area in Subang Regency

| NAME OF PROSPECT | TYPE OF SURFACE MANIFESTATION | NEARBY POWER PLANT | LOCATION | SURFACE TEMPERATURE (°C) | GEOTHERMOMETER TEMPERATURE (°C) | TYPE OF FLUID MEASURED | FLOW RATE (l/s) | CHEMICAL CONTENT |
|---|---|---|---|---|---|---|---|---|
| Cisolok (33) | Spouting springs | - | Cisolok River, 70 km west of Sukabumi | | 160-200 | | | |
| | 1 | | | 94.6 | | Liquid | 16 | 7.55 |
| | 2 | | | - | | Liquid | 0.1 | - |
| | 3 | | | 96.8 | | Liquid | 5 | 7.55 |
| | 4 | | | 95.2 | | Liquid | 16 | 7.3 |
| | 5 | | | 98.8 | | Liquid | 4.9 | 7.69 |
| Cisukarame (34) | Hot Springs | - | 6 km of Cisolok | 70-95 | 160-200 | Liquid | | 7.7 |
| Santa (35) | Hot Springs with iron oxide deposit around the springs | - | | | 130 | Liquid | | |
| Cikundul-Cimandiri (36) | Hot Springs with sulfur deposits around it | - | | | 100-140 | Liquid | | |

Figure 22 Geothermal manifestation area in Sukabumi Regency

| NAME OF PROSPECT | TYPE OF SURFACE MANIFESTATION | NEARBY POWER PLANT | LOCATION | SURFACE TEMPERATURE (°C) | GEOTHERMOMETER TEMPERATURE (°C) | TYPE OF FLUID MEASURED |
|---|---|---|---|---|---|---|
| Congeang-Cileungsing, G. Tampomas (37) | Hot Springs with salt | - | | | 180-240 | |
| | - Cipanas I Hot Spring | | Cipanas | 50 | | Liquid |
| | - Cipanas II Hot Spring | | Cipanas | 44 | | Liquid |
| | - Ciuyah Hot Spring | | Ciuyah | 38 | | Liquid |
| | - Ciledre Hot Spring | | Ciledre | 38 | | Liquid |
| | - Cileungsing Hot Spring | | Cileungsing | 47 | | Liquid |
| | - Cihaseum Hot Spring | | Cihaseum | 34 | | Liquid |
| | Silica Sinter and iron oxide | | | | | |

Figure 23 Geothermal manifestation area in Sumedang Regency

| NAME OF PROSPECT | TYPE OF SURFACE MANIFESTATION | NEARBY POWER PLANT | LOCATION | SURFACE TEMPERATURE (°C) | GEOTHERMOMETER TEMPERATURE (°C) | TYPE OF FLUID MEASURED | FLOW RATE (l/s) | CHEMICAL CONTENT | HEAT IN PLACE |
|---|---|---|---|---|---|---|---|---|---|
| Kawah Karaha (38) | Vulcanic Crater | - | Regency Garut includes Kecamatan Pangatikan & Kecamatan Karang tengah (Regency. Garut), Kecamatan Kadipaten & Kecamatan Ciawi (Regency Tasikmalaya) | | >250 (~350) | | | | |
| | Fumarol | | | | | Vapor | | | |
| | Hot Ground | | | | | Vapor | | | |
| | Altered Ground | | | | | | | | |
| | Hot Springs | | | 91 | | Liquid | 1.6 | Sulphur | |
| Cipacing (39) | Hot Springs | - | Desa Cipacing Kecamatan Pagerageung | | 259-271 | Liquid | | | |
| | Travertine | | | | | | | | |
| Cigunung (40) | Hot Springs : | - | Kampung Beubeudahan, Desa Cigunung, Kecamatan Parung | 33 | 180 | | | | 496.46 KW |
| | 1 | | | 59.5 | | Liquid | | pH: 6.25, HCO3 type | |
| | 2 | | | 56.4 | | Liquid | | pH: 6.25, HCO3 type | |
| | 3 | | | 49.4 | | Liquid | | pH: 6.44, HCO3 type | |
| | 4 | | | 60.7 | | Liquid | | pH: 5.98, HCO3 type | |
| Cibalong (41) | Hot Springs : | - | Kampung Cipanas, Desa Parung, Kecamatan Cibalong | | 180 | | | | 167.15 KW |
| | 1 | | | 49.7 | | Liquid | | pH: 5.73, Cl-HCO3 type | |
| | 2 | | | 46.1 | | Liquid | | pH: 5.29, Cl-HCO3 type | |
| Ciheuras-Cipatujah (42) | Hot Springs : | - | Kampung Cipanas Desa Cipanas Kecamatan Cipatujah | | 180 | | | | 269.85 KW |
| | 1 | | | 51.8 | | Liquid | | | |
| | 2 | | | 51.6 | | Liquid | | pH: 6.32, Cl-SO4 type | |
| | 3 | | | 50 | | Liquid | | pH: 5.5, Cl-SO4 type | |
| Galunggung (43) | Hot Springs : | - | Kampung Cipanas Desa Linggarjati Kecamatan Sukaratu | 60 | 180 | | | pH: 5.1, Cl-SO4 type | 1542.62 KW |
| | 1 | | | 50 | | Liquid | 2 | pH: 6.37, SO4 type | |
| | 2 | | | 60 | | Liquid | 3 | pH: 6.51, SO4 type | |
| | 3 | | | 60 | | Liquid | 3 | pH: 6.45, SO4 type | |
| | 4 | | | 61 | | Liquid | 3 | pH: 6.51, SO4 type | |
| | Fumarol | | | | | Vapor | | | |
| | Solfatara | | | | | Vapor | | | |
| | Altered Ground | | | | | | | | |
| | Vulcanic Crater | | | | | | | | |

Figure 24 Geothermal manifestation area in Tasikmalaya Regency

## 2.1 Potential Hot Springs for Geothermal Applications

Of geothermal manifestation types, hot spring is more common to be used for applications. Therefore, we set the criteria for potential resource from manifestation is hot spring with good temperature which is considered to be potential for use of low-medium enthalpy.

Table below summarizes hot springs temperature, flow rate, and heat load (MW)

| No. | Surface Manifestation | Surface Temperature (°C) | Flowrate (L/s) | Heat Load (MW) |
|---|---|---|---|---|
| 1 | Ciracas Hot Springs | 41.6-46 | 0.2 | 0.04 |
| 2 | Batu Gede Hot Springs | 42.1-45.5 | 0.2-1 | 0.11 |
| 3 | Kawah Domas Hot Springs | 85.5 -91.1 | 0.3-2 | 0.41 |
| 4 | Kancah Hot Springs | 31.1-34.5 | 3.3-5.1 | 0.57 |
| 5 | Cimanggu Hot Springs | 34.1-35.2 | 2.3-2.85 | 0.37 |
| 6 | Maribaya Hot Springs | 45.1-46.6 | 0.23-1.1 | 0.13 |
| 7 | Patuha Hot Springs | 35-83 | 2-15 | 2.07 |
| 8 | Cimanggu Hot Springs | 40-55 | 7.82-15.87 | 2.33 |
| 9 | Rancawalini Hot Springs | 40-55 | 7.17-15.87 | 2.27 |
| 10 | Cibuni Crater Hot Springs | 85-90 | >3 | 1.06 |
| 11 | Ciwidey Hot Springs | 70-90 | >4 | 1.30 |
| 12 | Wayang Windu Hot Springs | 39-66 | 15 | 3.25 |
| 13 | Kawah Kamojang Hot Springs | 90-93 | 2 | 0.74 |
| 14 | Kawah Hujan Hot Springs | 94 | 2 | 0.76 |
| 15 | Citepus Hot Springs | 55-60 | 2 | 0.47 |
| 16 | Ciseeng Warm Springs | 44.3 | 0.5 | 0.09 |
| 17 | Cibodas Hot Springs | 65.7 | 0.13 | 0.04 |
| 18 | Ciherang Hot Springs 1 | 39.3 | 0.03 | 0.00 |
| 19 | Ciherang Hot Springs 2 | 35.3 | 0.17 | 0.02 |
| 20 | Cisaketi Hot Springs 3 | 42.1 | 0.33 | 0.06 |
| 21 | Cipanas Karang Hot Springs | 71.2 | 0.07 | 0.02 |
| 22 | Muhinin Hot Springs | 40 | 0.03 | 0.00 |
| 23 | Sarimaya Hot Springs | 61.2 | 0.08 | 0.02 |
| 24 | Cipanas Cikuluwung Hot Springs | 47.2 | 0.15 | 0.03 |
| 25 | Cihideung Hot Springs | 46 | 0.18 | 0.03 |

| No. | Surface Manifestation | Surface Temperature (°C) | Flowrate (L/s) | Heat Load (MW) |
|---|---|---|---|---|
| 26 | Kawah Ratu-G.Salak Hot Springs 1 | 45.9 | 2 | 0.38 |
| 27 | Kawah Ratu-G.Salak Hot Springs 2 | 40.3 | 1 | 0.17 |
| 28 | Panulisan Warm Springs | 44-52 | 2 | 0.40 |
| 29 | Tanggeung-Cibungur-Cibuni Hot Spring 1 | 70.5 | 2 | 0.58 |
| 30 | Cipanas-Pacet Warm Springs | 40 | 0.8 | 0.13 |
| 31 | G.Kromong Hot Springs | 57 | 4 | 0.94 |
| 32 | Talaga Bodas Hot Springs | 68.1 | 7 | 1.95 |
| 33 | Kawah Mas Hot Springs | 79 | 0.17 | 0.05 |
| 34 | Kawah Manuk Hot Springs | 65 | 0.17 | 0.05 |
| 35 | Cibeureum Leutik Hot Springs | 32 | 0.25 | 0.03 |
| 36 | G. Masigit-Guntur Hot Springs | 45 | 2 | 0.37 |
| 37 | Cilayu Hot Springs | 61 | 1 | 0.25 |
| 38 | Subang Hot Springs 1 | 60.5 | 2 | 0.50 |
| 39 | Subang Hot Springs 2 | 60.8 | 0.5 | 0.13 |
| 40 | Subang Hot Springs 3 | 60.9 | 0.5 | 0.13 |
| 41 | Subang Hot Springs 4 | 60.7 | 0.5 | 0.12 |
| 42 | Cibingin Hot Springs | 54.2 | 3 | 0.67 |
| 43 | Ciater Hot Springs | 44-46.9 | 2 – 15 | 1.60 |
| 44 | Batu Kapur Hot Springs | 39.4-40.1 | 2.2 – 3.9 | 0.50 |
| 45 | Cisolok Hot Springs 1 | 103 | 10 | 4.13 |
| 46 | Cisolok Hot Springs 2 | 99 | 10 | 3.98 |
| 47 | Cisolok Hot Springs 3 | 82 | 10 | 3.33 |
| 48 | Cisolok Hot Springs 4 | 101 | 10 | 4.05 |
| 49 | Cisolok Hot Springs 5 | 96 | 10 | 3.87 |
| 50 | Kawah Karaha Hot Springs | 91 | 1.6 | 0.59 |
| 51 | Galunggung Hot Springs 1 | 50 | 2 | 0.41 |
| 52 | Galunggung Hot Springs 2 | 60 | 3 | 0.74 |
| 53 | Galunggung Hot Springs 3 | 60 | 3 | 0.74 |
| 54 | Galunggung Hot Springs 4 | 61 | 3 | 0.75 |

After looking into the temperature data of manifestations, we learn that there are some geothermal prospects which have relatively higher temperature than other geothermal prospects. Two of them are Cisolok and Cisukarame geothermal prospects can be examples to learn the characteristics of the manifestation (i.e. spouting hot spring, hot pool, and bubble hot spring). Herewith the description of Cisolok and Cisukarame.

### 2.1.1 Cisolok Hot Springs

The geothermal manifestation appears at 106°27'13.4" E and 6°56'0.5" S in the Cisolok River, 70 km west of Sukabumi Regency or about 170 km from Bandung. At present, the geothermal manifestation of Cisolok is used as public bathing place.

The thermal water discharging in Cisolok River has high temperature near boiling temperature, with neutral pH and relatively high discharge rate. Along the river bank around the hot spring, there is hydrothermal surface alteration dominated by silica sinter and travertine.

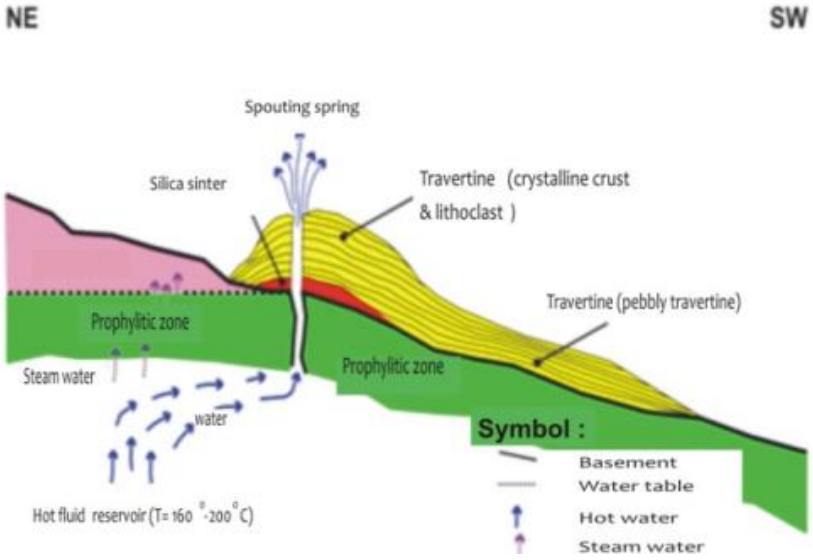


Figure 25 Sketch of NE-SW sections of geothermal manifestations along Cisolok Rivers (without scale). Reference: Mandradewi, W., and Herdianita, N.R. (2010)

The survey to Cisolok indicates that there are at least six hot springs discharging continuously in Cisolok River. These manifestations are classified as spouting springs because of artesian discharge. The discharging thermal water then mixes with stream water having temperature of about 28°C and results in a temperature of 34°C in the mixed water (Mandradewi, W., and Herdianita, N.R. (2010)).


Figure 26 Spouting Springs (MAP_CSK_1)

1. Spouting Spring (MAP_CSK_1)

   Coordinate (UTM) : X= 0660552
   Y= 9233322

   Elevation : 93 m

   (a). Temperature : 94,6°C

   pH : 7,55

   Diameter : 10 cm

   Area : 0,00785 $m^2$

   Averaged velocity : 2,06 m/s

   Debit : 0,016223 $m^3/s$

   (b). Diameter : 2 cm

   Area : 0,000314 $m^2$

   Averaged velocity : 0,33 m/s

   Debit : 0,000105 $m^3/s$

   (c). Temperature : 96,8°C

   pH : 7,55

   Diameter : 10 cm

   Area : 0,00785 $m^2$

   Averaged velocity : 0,633 m/s

   Debit : 0,004972 $m^3/s$

   River: Direction from north to the south

   Temperature : 39,8°C

   pH : 7,78

Averaged velocity : 0,3 m/s;

Wide : 5,9 m

Debit : 354 l/s

Figure 27 Spouting spring (MAP_CSK_3)

We eliminate MAP_CSK_2 and MAP_CSK_3 because the flow rate is relatively small.

1. Spoutting Spring (MAP_CSK_4)

Coordinate (UTM) : X= 0660570
Y= 9233370

Elevation : 78 m

Temperatur : 98,8°C

pH : 7,69

DHL : 108,7 mV

Diameter : 5 cm

v : 2,5 m/s

Debit : 0,004906 $m^3/s$

Figure 28 Picture showing people bathing in stream with the sputing spring in the background


Figure 29 Spouting springs in Cisolok

### 2.1.2 Cisukarame Hot Springs

Cisukarame is located about 6 km north of Cisolok. A hot pool occurs in the middle of a rice field in Cisukarame.

1. Hotspring (MAP_SKR_1)

   Coordinate (UTM) : X= 0664549

Y= 9237694

Elevation : 265 m

Air Temp : 30,2°C

Temperature : 73,7°C

pH : 6,84

DHL : 17,3 mV

Diameter : 40 cm

Averaged velocity : 0,6 m/s

Debit : 0,07536 $m^3/s$

Wide : 2,5 m

It flows from north to the south

Figure 30 Hotspring (MAP_SKR_1)


Figure 31 Bubble hotspring (MAP_SKR_3)

2. Bubble Hotspring (MAP_SKR_3) – Figure 31

| | |
|---|---|
| Coordinate (UTM) | : X= 0664542 |
| | Y= 9237698 |
| Elevation | : 264 m |
| (a). Temperature | : 87°C |
| pH | : 6,72 |
| DHL | : 25 mV |
| Diameter | : 90 cm |
| (b). Temperature | : 80,8°C |
| pH | : 6,57 |
| DHL | : 33 mV |
| Wide | : 50 cm |
| Thickness | : 12 cm |
| Velocity | : 0,6 m/s |
| Debit | : 36 l/s |

Figure 32 Hotpool (MAP_SKR_4)

3. Hotpool (MAP_SKR_4)

| | |
|---|---|
| Coordinate (UTM) | : X= 0664551 |
| | Y= 9237715 |
| Elevation | : 264 m |
| Temperature | : 78,2°C |
| pH | : 6,54 |
| DHL | : 36,1 mV |
| Diameter | : 4,2 m |

Figure 33 (MAP_SKR_6)

4. Boiling Hotspring (MAP_SKR_6)

| | |
|---|---|
| Coordinate (UTM) | : X= 0664572 |
| | Y= 9237695 |
| Elevation | : 265 m |
| Temperature | : 92,3°C |
| pH | : 8,1 |
| Diameter | : 20 cm |
| Averaged velocity | : 0,1 m/s |
| Debit | : 0,00314 $m^3/s$ |

## 2.2 ONSHORE NORTHWEST JAVA BASIN (POTENTIAL HOT SEDIMENTARY AQUIFER?)

### 2.2.1 Regional Geothermal Resource Estimation

Introduction

Geothermal systems in sedimentary basins has been recognized for quite a long time (e.g. Rybach &, 1981) with the assessments of their characteristics and resources and their exploration methodology being mostly distinguished from those of conventional volcanic hydrothermal (e.g. Cooper & Beardsmore, 2010). This is due to their fundamentally different types of heat source and heat transfer mechanism; the former has a heat source derived from high regional heat flow, insulating sediments, and/or heat-producing radiogenic rocks and is usually dominated by conduction, whereas the latter is related to magmatic activities and is dominated by natural convective water circulation (Lund, 2007). Consequently, most geothermal systems in sedimentary basins display lower average temperature than their volcanic hydrothermal counterparts at any equal depths (< 150 °C; Rybach, 1981), and hence their resources fit the criterion of being low to medium enthalpy. This should also be the case for onshore North West Java Basin, which, due to reasons explained below, may become a suitable candidate for another study on the geothermal system in a sedimentary basin.

Previous studies concerning the possibilities of both the presence of economic geothermal resource in the area of onshore North West Java Basin (e.g. PT LAPI ITB, 2014; Putra, 2015) as well as its utilization schemes (e.g. Taqwim, 2014) have been carried out, with all of them showing positive results. The studies aimed at predicting the presence and magnitude of the geothermal resource in this basin have however been either too specific, for example PT LAPI ITB's (2014) report which aimed at the exploration of Hot Sedimentary Aquifer geothermal play for utilization in Jakarta area, or too regional like that of Putra's (2015) study which was focused on the modelling of regional thermal structure. In the former case, only temperature-permeability data from wells around the target area were used to achieving the goal of locating the depth and stratigraphy of a prospective reservoir. In contrast, the latter study used a modelling approach based on heat-flow density datasets from wells over the entire basin, but the resource base was calculated from the resulting modelled temperature instead of by directly utilizing any available well temperature-at-depth values. Knowledge of the geothermal resource base in particular is essential for establishing the necessary foundations should further exploration campaign(s) be undergone and if future utilizations are to be realized at a desired target location. However, maximizing the direct

use of available data is also more preferable for determining the magnitude of the resource at that specific location rather than relying on model-derived estimates. Thus, the remainder of this part of the report is dedicated to a detailed elaboration of the systematic procedures undertaken to perform the estimation of the gross geothermal resource base of an area within the onshore North West Java Basin based on available data. The end product of this resource assessment is intended for a prediction of the feasibility heat extraction from a prospective aquifer(s) in the basin by the Frisian Flag factory as our initial desired target market.

## The Onshore Northwest Java Basin

The onshore North West Java Basin is situated in the northwestern part of the island of Java. It encompasses three major provinces (Banten, West Java, and the Capital City of Jakarta) as well as several regencies (**Fig. 34**). The basin is known to host hydrocarbon resources (**Fig. 35B**), the reserves of which has been confirmed through commercial drilling and exploitation activities by PT PERTAMINA, a state oil company (Suryantini, 2007). Given the location of Frisian Flag, it is safe to say that we will have no conflict concerning the area for heat extraction, since the exploitation activities are mostly conducted to the eastern sector of the basin rather than in the vicinity of the Capital City of Jakarta.


Figure 34 Geographic location of the study area, showing the areal extent of the onshore part of the North West Java Basin and the approximate location of the geothermal market target.

## General Geological Setting

Physiographically, the onshore North West Java Basin lies on the Coastal Plain of Jakarta (Suryantini et al., 2006). It possesses a number of general geological and structural features

that are summarized in **Figure 35.A** and **35.B**. The basin is bounded by a series of thrust faults to its south. In addition, several compartments which are comprised of a series of sub-basins (areas of deep basement rock) and basin highs (areas where the basement is shallower) can be found to constitute the overall basin's geometry (Suryantini, 2007; PT LAPI ITB, 2014; Putra, 2015). Each of these compartments is bounded to its sides by deep-seated basement faults.

**Figure 36** displays a stratigraphic column of the basin. As **Figure 36** shows, the basin's formation was initiated as early as the Early Oligocene (about 35 Myr BP) as a sequential rifting process. The rifting was terminated at Late Oligocene (about 25 Myr BP). The entire rifting sequence is what has likely induced the basement compartmentalization process and created the bounding faults described above. A subsequent subsidence not related to rifting took place at Early Miocene (the Sag Phase). The final phase of basin evolution takes the form an uplift and erosion due to compression, which is related to the current tectonic setting of Java, i.e. by West-East oriented subduction zone along the southern part of the island. Each stage of the basin's evolution was also accompanied by the deposition of sedimentary units which are underlain by an igneous and metamorphic basement (**Fig. 35**). The types of lithology formed during the deposition are governed by the depositional environment at their respective age, which ranges from shallow marine to non-marine ones. Systematically, the oldest basin fill is the Jatibarang Formation, which is comprised of volcanic rocks dating from Late Eocene – Early Oligocene. It is overlain by the Lower Cibulakan Formation of Late Oligocene – Early Miocene age, which is composed of two members, i.e. the Talang Akar (sandstones with major shale intercalations) and the Baturaja limestone. The Upper Cibulakan Formation (Early - Mid Miocene) consists of shale with sandstone intercalations and some carbonate buildups. The overlying, Late Miocene Parigi Formation is comprised entirely of carbonate buildups and reef limestones. The youngest Tertiary sedimentary formation to exist in the basin is the Cisubuh Formation, all of which is constituted by shale. Finally, most of the basin's surface is covered by alluvium deposits, with tertiary sediments and tertiary-quartenary volcanic products cropping out at the southern, western, and central parts of the basin. A picture of the depth extent of each formation is given in a cross-section in **Figure 37**.

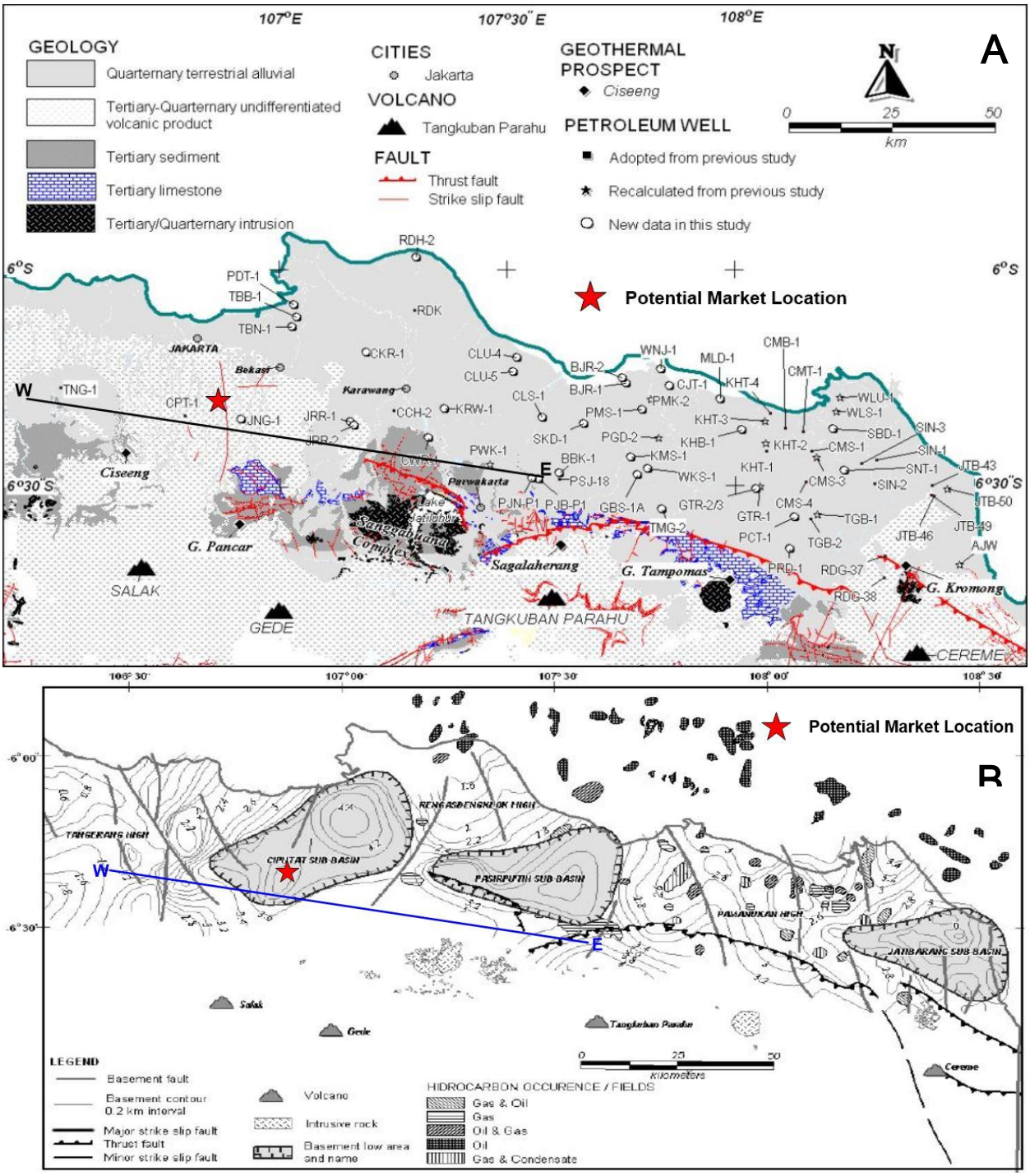


Figure 35 Map showing (A) the distribution of superficial lithology, other geological elements, and distribution of well data used in Suryantini's (2007) study, (B) major compartments, basement faults, contours of basement depth, and the distribution of hydrocarbon types of the onshore North West Java Basin.

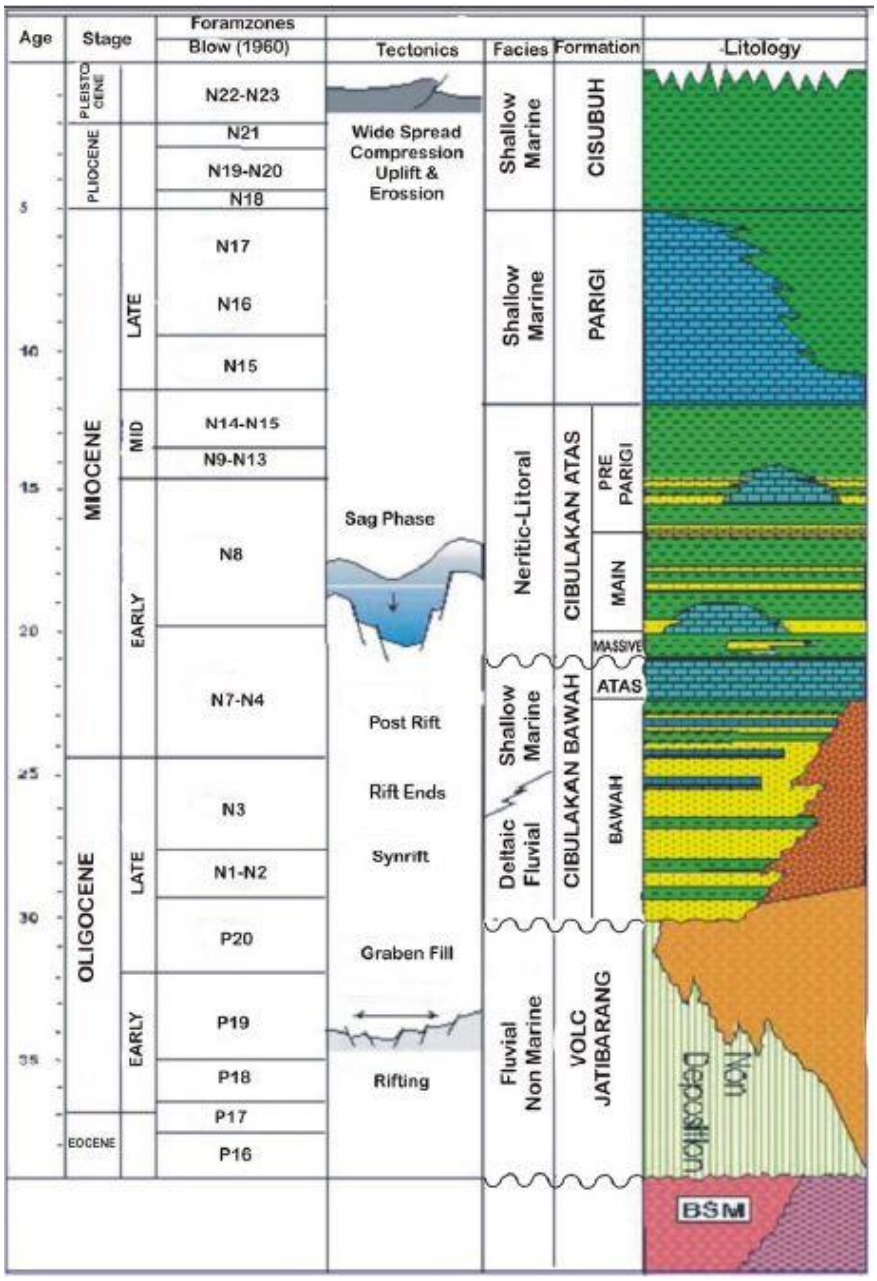


Figure 36 Stratigraphic column of the onshore North West Java Basin (Arpandi and Patmosukismo, 1975 with modifications by PT LAPI ITB, 2014).

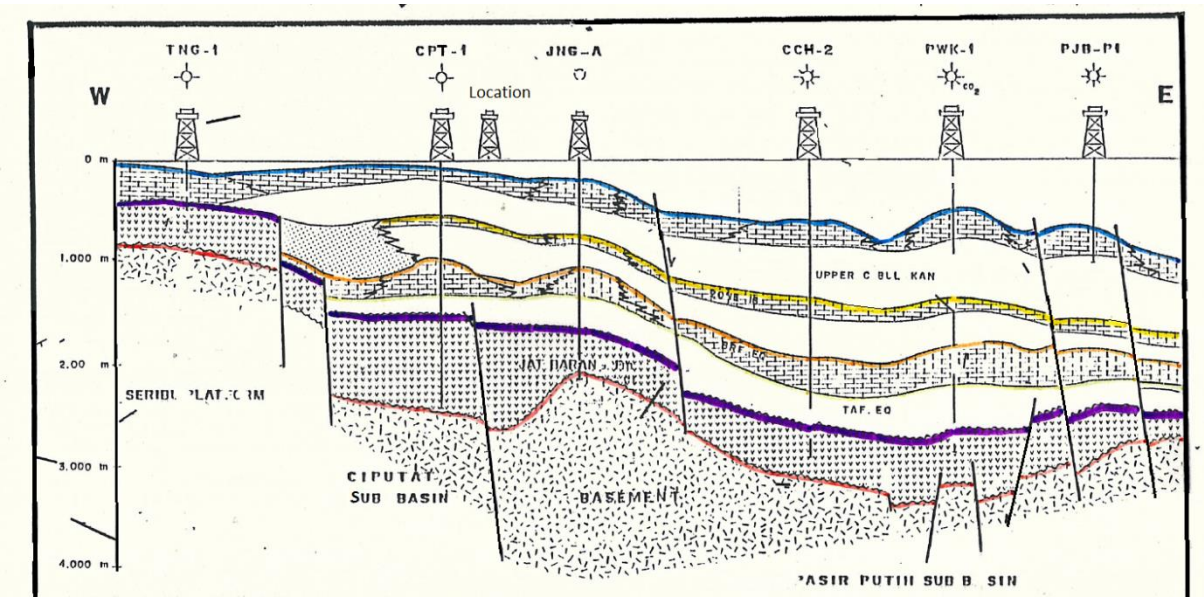


Figure 37 A geological cross-section along the profile line drawn in **Figure 35**. The top of a specific formation or a member, other than Cisubuh Formation which becomes the topmost layer, is marked with different colors; blue: Parigi Formation, yellow: main member of the Upper Cibulakan Formation, orange, light yellow: Baturaja, Talang Akar members of the Lower Cibulakan Formation, purple: Jatibarang Formation, and Pink: Basement. The approximate location of the target market location is shown using a well symbol.

## Thermal Regime

The onshore North West Java Basin has become a subject or included in a number of studies in terms of its thermal regime, e.g. Thamrin (1985), Suryantini et al (2006), Suryantini (2007), and Putra (2015). A heat-flow density (HFD) map of the entire basin was constructed by Suryantini (2007) and is shown in **Figure 38**, along with their measurement points. From **Figure 38**, we can observe that HFD varies greatly between places in the basin. The HFD values range from below 80 $mW.m^{-2}$ at several locations at the peripheries of Ciputat and Jatibarang Sub-basins, to over 200 $mW.m^{-2}$ at a location on the southern boundary of the Pasirputih Sub-basin. HFD values that range between 70 $mW.m^{-2}$ and ≈90 $mW.m^{-2}$ are distributed over the Pamanukan High area. In addition, it is interesting to see that the magnitude of HFD correlates with the distribution of hydrocarbon types (**Fig. 38B**). The areas beneath which hydrocarbons are present as two-phase fluids (oil and gas, gas and oil, or gas and condensate) correspond to HFD values between 70 $mW.m^{-2}$ and ≈90 $mW.m^{-2}$, like that around the Pamanukan High area. In an area where HFD reaches over 150 $mW.m^{-2}$, i.e. that located on the southern edge of the Pasirputih Sub-basin, hydrocarbon is present in the form of gas. The high HFD values recorded in this area conforms to the volcanic front interpreted from magnetic data, such that these extremely high values give the impression of being representative of a magmatic activity to the south (i.e. the Tangkuban Parahu volcano,

Fig. 35). As for the area surrounding the market target's location, the HFD value is also high (≈140 mW.m$^{-2}$), suggesting that the temperature at depth there may be higher than most of the other areas' and that there might be a significant amount of heat stored beneath.

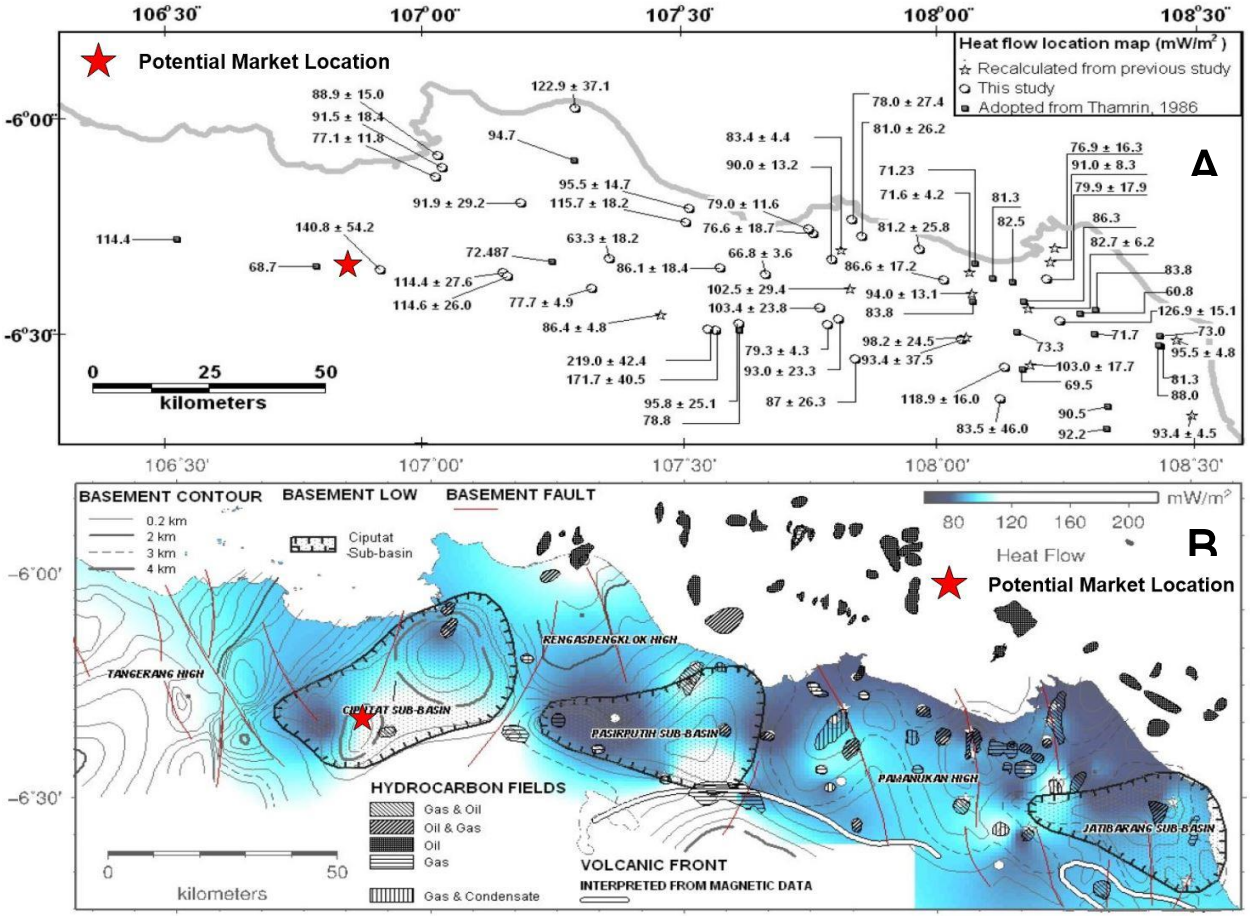


Figure 38 (A) Point-map and (B) Contour map of heat flow of Onshore NW Java Basin. The basin structure map is also superimposed on the contoured heat flow map (Suryantini, 2007).

## Data and Methodology

Our goal was to estimate the geothermal resource base of a portion of the onshore North West Java Basin. Other areas of the basin, despite having more number of wells, are not considered since no thermal data are available for these wells. The attempts to perform this estimation were based on two approaches: (1) Obtaining any available temperature-at-depth values from hydrocarbon wells in the area, the data of which were derived from the PT LAPI ITB (2014) report for use to create temperature-at-depth and stored heat-in-place maps, and (2) Using the results of Putra's (2015) study for the resource base of individual sub-basins down to a certain depth based on reasonable economic drilling depth. Both approaches closely resemble that used in estimating the regional resource base for Enhanced Geothermal Systems (EGS) play (e.g. Blackwell et al., 2007; Beardsmore et al., 2010). Since, like that of typical EGS, the basin under investigation does not possess any

observable surface manifestations, the use of the aforementioned approaches should be reasonably appropriate. Consequently, the resource calculations did not take into account the energy associated with geothermal fluids. The subsurface temperature data for the first approach were obtained from Bottom Hole Temperature (BHT) and Drill Stem Test (DST) temperature values previously collated in PT LAPI ITB (2014) for 13 hydrocarbon wells (**Fig. 39**). The original report contained the complete listing of each temperature value, measurement depth, and calculated thermal gradient.

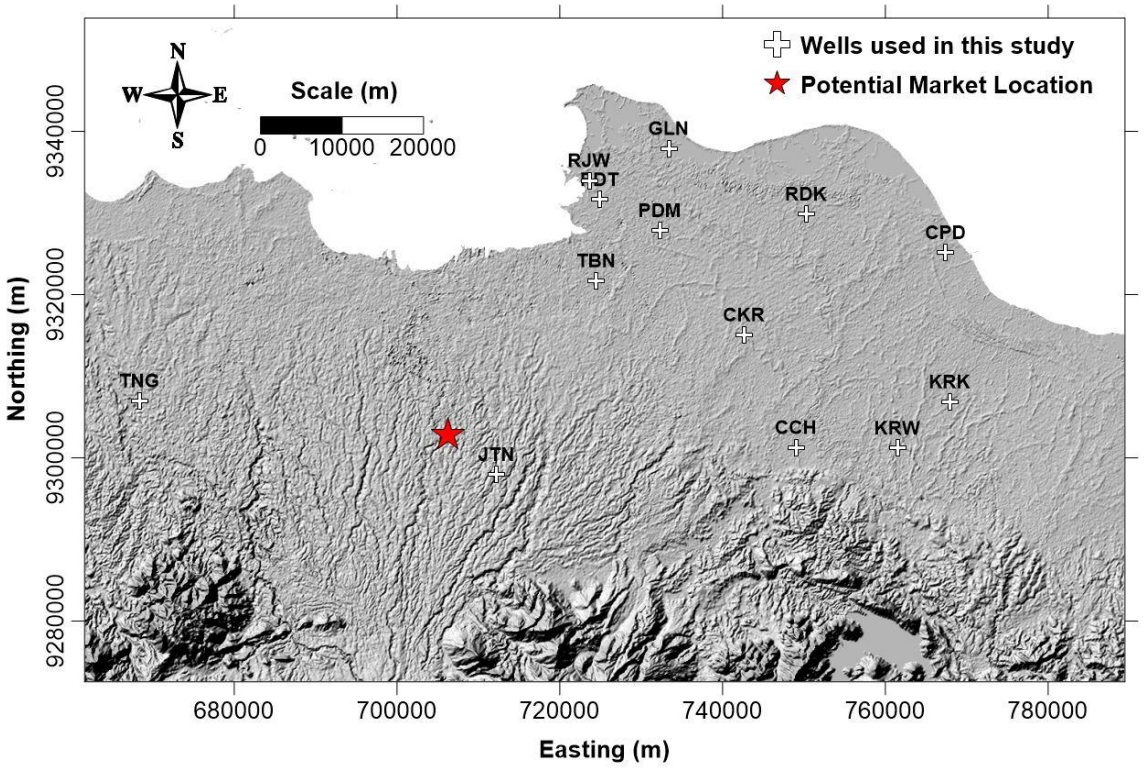


Figure 39 Distribution of hydrocarbon wells whose temperature data were directly used for temperature-at-depth and resource-at-depth calculations in this study.

In the first approach, we created averages of the temperatures for each 1000 meter depth interval, from 0 to 3000 meters, from which we also recalculated the thermal gradients. No temperature value was recorded below 3500 meter depth, so it was decided to use 3000 meters as the maximum depth for our calculations. In addition, a few wells also lack temperature data for one or more of the intervals. The choice of the depth interval was somewhat arbitrary, but could be partly justified considering the nature of the original BHT values. Standard correction procedure (e.g. Horner Plot) could not be performed due to the lack of cessation time of mud circulation data (PT LAPI ITB, 2014), causing the observed uncorrected BHT values to display quite strong fluctuations. Therefore, we expected that by using a relatively great depth interval the more BHT and DST values would be included in the averaging procedure, so that these fluctuations could be reduced to a degree. The

averaged temperatures-at-depth were subsequently utilized as inputs to the calculation of geothermal resource base, the formula of which was adopted from Muffler & Cataldi (1978):

$$H = \rho \times C_p \times (T_z - T_0) \times \Delta x \times \Delta y \times \Delta z \qquad Eq.(1)$$

Where $H$ is the stored thermal energy within a volume of rock, $\rho$ and $C_p$ are rock density (kg.m$^{-3}$) and heat capacity (J.kg$^{-1}$.$^0$C$^{-1}$), $\Delta x, \Delta y, \Delta z$ are the grid sizes (m), and $T_z$ and $T_0$ are the temperatures at a particular depth and the surface ($^0$C), respectively. $T_z$ is the averaged values of temperature within each 1000 meter depth interval, and the surface temperature was assumed to be 28 $^o$C. The values of $\rho$ and $C_p$ were taken to be 2500 kg/m$^3$ and 1000 J/kg, following that of Blackwell et al. (2007). The lateral grid sizes $\Delta x$ and $\Delta y$ followed those of Putra (2015), i.e. 2000 meters each and the vertical grid $\Delta z$ is 1000 meter, following the depth interval used.

As for the second approach, a subsurface temperature distribution model of Putra (2015) was directly utilized to calculate the stored thermal energy for individual compartments of the onshore North West Java Basin, i.e. Ciputat, Pasirputih, and Jatibarang Sub-basins. This temperature distribution model was generated through a 3-D numerical finite-difference modeling of steady-state conductive heat transfer. This approach was taken due to the unavailability of well temperature data in the central to easternmost parts of the basin. All other calculation parameters remain similar, the only exception being that now the temperature is readily available at every grid node within the boundaries of each sub-basin so that the vertical grid size reverts to only 100 meter.

## Results and discussions

While the averaged temperatures became the primary inputs to the calculation of stored thermal energy using Eq. (1), the averaged thermal gradients were used to calculate temperatures-at-depth for each 500 meter interval, from 0 to 3000 meters. The original surface temperature used to determine thermal gradients in both PT LAPI ITB's (2014) report and this work was 25 $^o$C, however to calculate the absolute temperatures-at-depth a value of 28 $^o$C–the same value used in thermal energy calculation, was taken instead. The chosen surface temperature followed that assigned to the resource base calculation, by considering that the average of the regression-derived surface temperature in Suryantini (2007) actually lies closer to this value. The subsurface temperature-at-depth and stored thermal energy maps were generated using the Golden Software's Surfer 11 ™ through the default Kriging interpolation method and are shown in **Figure 41** and **40**. The calculated stored thermal energies for each sub-basinal compartment of the onshore North West Java Basin are listed in **Table 1.**

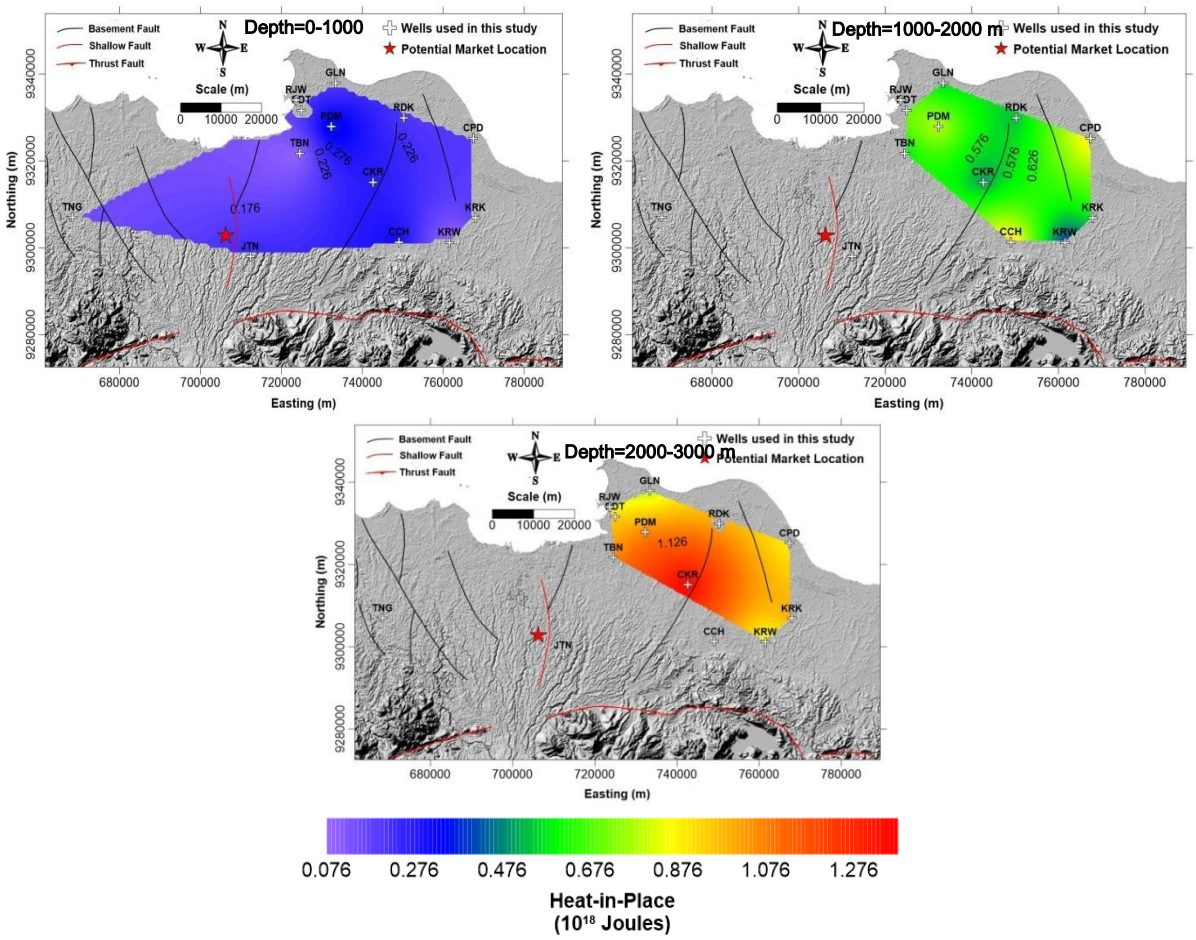


Figure 40 Subsurface stored heat energy maps constructed by interpolating calculated values using Eq. (1) and the average temperatures over 1000 meter depth intervals.

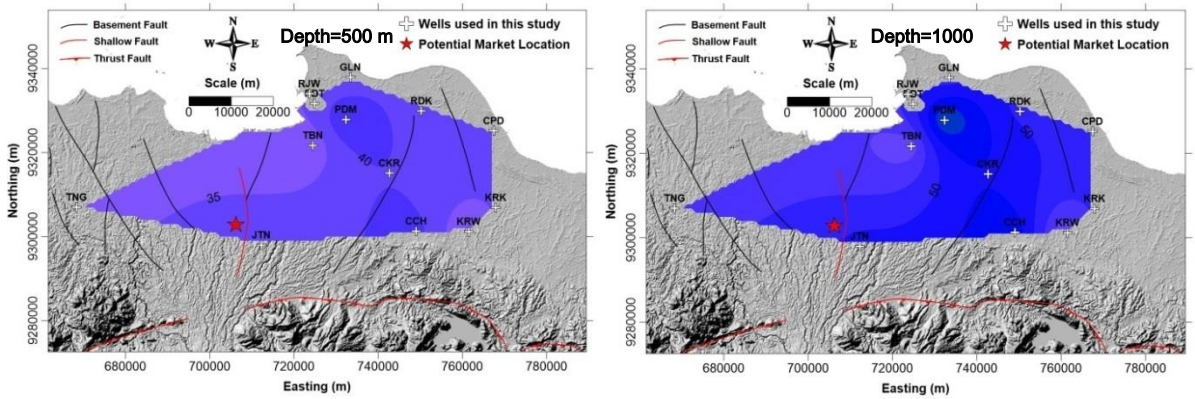

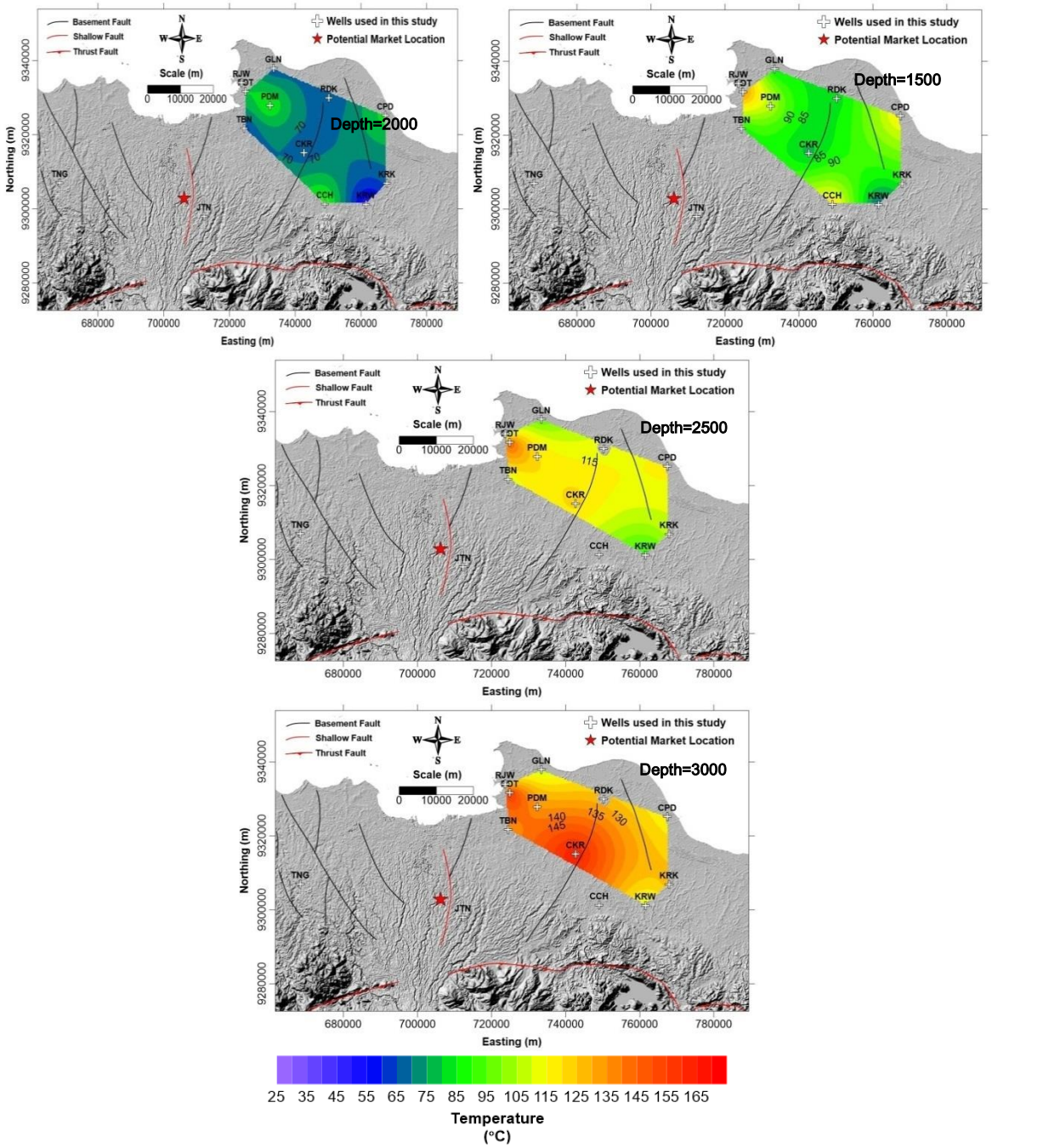


Figure 41 Subsurface temperature maps constructed by interpolating average temperatures calculated from well BHT and DST data compilation of PT LAPI ITB (2014).

Table 1 Estimated stored heat-in-place for each sub-basinal compartment of the onshore North West Java Basin using Eq. (1) and subsurface temperature model of Putra (2015).

| NO | GEOTHERMAL PROSPECT | INCLUDED CITIES/REGENCIES | LOCATION | NET SURFACE AREAL EXTENT (km²) | HEAT IN PLACE (Joules) |
|---|---|---|---|---|---|
| 1 | Ciputat Sub-basin | The Capital City of Jakarta | Onshore North West Java Basin | 978.64 | 5.43E+20 |
| | | Bekasi | | | |
| | | Depok | | | |
| | | Cikarang | | | |
| 2 | Pasirputih Sub-basin | Karawang | | 745.39 | 4.13E+20 |
| | | Purwakarta | | | |
| 3 | Jatibarang Sub-basin | Cirebon | | 571.83 | 3.17E+20 |
| | | Indramayu | | | |

From **Figure 40** and **41**, we can observe that the highest temperatures, and consequently greater amount of geothermal resource base (stored heat-in-places) at shallower depth ranges (<2000 meters) are mostly found at the vicinity of wells PDT, PDM, and CCH. At depths greater than 2000 meters, however, temperatures beneath the well CKR increases significantly, causing the stored heat to be greater at that location than any other areas where the wells are distributed.

The area surrounding well CCH was identified as the location where a heat refraction phenomenon, by which heat preferentially flows along the more conductive basement rock, occurred (Putra, 2015). According to the author, the phenomenon was caused by the transition between sub-basins (i.e. the Ciputat and Pasirputih Sub-basins), which are separated by a narrow basement high (the Rengasdengklok High, which somewhat acts as a ridge). Thus, the high temperature might have been induced by this phenomenon. On the other hand, **Figure 35B** shows that the well CKR location is actually close to a basement fault, which implies that the sharp increase in temperature at greater depths might be attributed to advective heat transfer by groundwater circulation through this fault. Nevertheless, these explanations should not be overrated as the wells PDT and PDM do not seem to experience a similar condition to any of the other two wells. More well data, geological, and hydrological information need to be collected in order to increase our confidence in interpreting the possible causes to the observed subsurface thermal behaviour.

**Table 1** displays the calculated heat in places for the sub-basins. Calculations concerning the heat in places of specific reservoir formations (aquifer) are contained in the next part of the resource assessment report. The Ciputat Sub-basin is shown to possess the greatest amount of stored thermal energy. Aside from the sheer magnitude of areal extent of this sub-basin, the Ciputat Sub-basin also has the deepest basement of all other sub-basins (**Fig 35B**). This sub-basin, being the deepest, is equal to saying that it has the thickest sedimentary filling, which, according to Cooper & Beardsmore (2010) acts as an insulating unit; the thicker this unit becomes the greater the calculated stored heat-in-place is. Nevertheless, the estimated resource base should only serve as a background value rather

than an exact one, since the temperature model was generated using the assumption of conductive heat transfer only for the entire basin. This is also true for the heat-in-place maps of **Figure 40**, from which their values were derived using averaged temperature at certain depth intervals. A more rigorous estimate would be allowed by the use of more sophisticated modeling procedure, including perhaps other heat transfer mechanisms, as well as by the availability of more detailed data concerning the geology and thermal regime of the basin.

### 2.2.2 Local Hot Sedimentary Aquifer Characterization

#### Introduction

Previously, we were concerned with the estimation if the geothermal resource base of the onshore North West Java Basin, the magnitudes of which were calculated separately for a limited area with well temperature data and the entire basin based on recent modelling results. The resulting stored heats for both are of gross values. Reservoir property analysis and resource characterization have not been performed so far. Therefore, we continue the discussion in this part by providing more detailed descriptions of a specific target deep aquifer (reservoir) within the basin. Specifically, an area outlined by the distribution of wells (**Fig. 39**) becomes the primary target. These descriptions are represented in the form of maps displaying the spatial distributions of parameters and properties considered to be vital to the estimation of the geothermal potential of a deep aquifer, i.e. its depth, thickness, temperature, porosity and permeability. It is to be noted that for the procedures described in the following sections, due to the problems of limited data availability, many literature values are used.

#### Methodology

Pluymaekers et al. (2012) provided a comprehensive description on the methodology of characterizing geothermal aquifers in sedimentary basin settings. For a deep sedimentary basin aquifer, from which geothermal heat is to be extracted, the most important properties to be characterized are its temperature, depth, thickness, porosity, permeability, and transmissivity (as the product of permeability and thickness). The geothermal production temperature of an aquifer can be estimated from the regional temperature gradient, since the water temperature will be equal to the surrounding aquifer rock temperature. Indeed, this assumption holds only when there is no significant vertical component of water flow, such that the temperature field is not distorted. Also, the aquifer layer needs to form a substantial horizontal extent as compared to lateral variations of its vertical thickness and elevation. Since knowledge on deeper subsurface flow fields is absent for the case of onshore North West Java Basin (Putra, 2015), we assume that these conditions are fulfilled and the aquifer

temperature is in equilibrium with its surroundings. The thickness and permeability of the aquifer must be known, since the product of the two results in transmissivity, the value of which a flow rate calculation is based on. In addition, it must be noted that the drilling cost increases as the depth of aquifer increases, however at shallower depths the aquifer may not have sufficiently high temperature to produce usable energy. It follows that all of the aforementioned factors must be taken into account when determining the potential of a hot sedimentary aquifer for geothermal uses.

In the following sections each of the reservoir properties mentioned above is discussed. For compactness, the area under consideration is taken to be the same as that of **Figure 39**. The choice is based on the relative location of the target market, by whom heat is going to be extracted (the Frisian Flag factory).

**Selection of Aquifers**

Pluymaekers et al. (2012) have described several criteria for choosing the most suitable candidates as potential aquifers to which we apply the characterization procedure. Aside for the criterion of a 10 $km^2$ minimum areal extent of the aquifer, which is met by every single formation within the basin, we decided to simply follow the recommendations of PT LAPI ITB (2014). The report suggests that the most potential reservoirs in the study area are of the Parigi Limestone Formation, Baturaja Limestone, and Talang Akar Sandstones (members of the Lower Cibulakan Formation). These reservoirs are described in the following:

1. Talang Akar Member of the Lower Cibulakan Formation

   The Talang Akar Formation is of late Oligocene to early Miocene age and is characterized as syn-rift to late rift continental style deposition. The lower part consists of sandstones, mudstones, minor coals, and tuffs of alluvial to deltaic origin. It has a total average thickness of 450 m. The basal unit is generally of poor reservoir quality, but the deltaic interval contains good reservoirs. The upper part consists of interbedded shale, limestone, coal, and sandstone and is ca. 300 m thick. This marine interval contains good reservoir rocks.

2. Baturaja Member of the Lower Cibulakan Formation

   This early Miocene Formation consists of well-developed limestone on the Seribu platform, along fault-controlled basement highs, and around basement highs. The best reservoirs are reef build-ups around basement highs that were exposed during sea-level low stands where secondary moldic porosity resulted from leaching of aragonite grains is very high. The reefs vary in thickness 30 - 45 m. The reservoir consists of wackstone and packstone and occasionally mud- or grainstone with high porosities up to 34%. Cut-

off values for determination of the reservoir properties of the Batu Raja Formation are generally high since the rock is believed to contain non-interconnected porosity (Crumb, 1989). The thickness varies between 150 and 390 m in the wells for which data were available. The high porosities of the Lower Batu Raja are of secondary origin and were formed by the diagenetic leaching of originally aragonitic skeletal material. In the offshore Krisna Field high porosities are distributed field-wide a a continuous lensoid body (Wight and Hardian, 1982). Wight and Hardian also showed that the thicker carbonate sections were developed away from the crest, behind the fringing reef edge.

3. Parigi Formation

   This unit was deposited during the (Middle Miocene – Early Late Miocene) in a shallow marine environment. Its thickness ranges from 27 meters to more or less 450 meters. It is predominantly composed of porous and fossiliferous light grey limestone, with very minor light brown dolomitic limestone and sandy limestone. Some calcareous shale and marl streaks can be observed in the lower part of the section. It presents good reservoir characteristics with very high secondary porosity and permeability (Arpandi and Padmosukismo, 1975).

Although the Parigi Formation presents good reservoir characteristics with its very high secondary porosity and permeability, it is mostly located in shallower depths (< 1000 meter), which does not meet the depth criterion of common geothermal deep aquifers (> 1000 meter; Ungemach et al., 2005). Also, the expected reservoir temperature would also be low, though individual geothermal gradients can be as high as ≈65 K/km within the formation. Instead, the Baturaja Limestone may be of more potential, since it is deep (> 1 km) and thick (150 to 390 meters). On the other hand, the Talang Akar sandstone is thin, ranging from 10 to 40 meters, and is intercalated with shales, despite having permeabilities of up to some ≈300 milliDarcies (PT LAPI ITB, 2014). Nonetheless, this thinness will mean an increase in lifetime due to thermal recharge during the development of heat extraction schemes (e.g. Poulsen et al., 2015), such that this aquifer remains to be potential for future use. Thus, the Talang Akar aquifer is considered in this report. Since the two aquifers are positioned vertically adjacent to each other, as they are both members of the Lower Cibulakan Formation, our following mapping and analyses of the aquifer properties and characteristics are confined to this particular formation. In all cases, the Kriging interpolation technique with default linear variogram model provided by Golden Software's Surfer™ 11 is applied to the mapping.

**Aquifer Depth and Thickness**

The depths to the top of Baturaja and Talang Akar aquifers and their thicknesses are obtained from PT LAPI ITB (2014) report, as well as Suryantini (2007) for wells whose depth and thickness values are not reported in the former. If a well does not possess values from any of the two references, the values obtained from the 3-D geological model of the onshore North West Java Basin constructed by Putra (2015) are used. Since the thickness values adopted from the last two references are of the entire sequence of the Lower Cibulakan Formation, the thickness of each aquifers derived from these references is equal to half of the Lower Cibulakan's. The depth and thickness values are listed in **Table 2**, while their spatial distribution is represented in maps shown in **Figures 42 to 45**.

Table 2 Tabulated depth-to-center and thickness values of the Baturaja and Talang Akar aquifers. Black-colored values denote those obtained from PT LAPI ITB (2014). Blue-colored values indicate those taken from the geological model used by Putra (2015). Red-colored values denote those obtained from Suryantini (2007).

| Well | Baturaja | | Talang Akar | |
|---|---|---|---|---|
| | Depth (m) | Thickness (m) | Depth (m) | Thickness (m) |
| CCH | 2550 | 300 | 2850 | 300 |
| JTN | 1280.5 | 371 | 1612 | 292 |
| CKR | 2124.5 | 289 | 2413.5 | 289 |
| PDM | 2007 | 298 | 2336.5 | 357 |
| PDT | 1871.1 | 237 | 2101.1 | 223 |
| RJW | 1800 | 200 | 2000 | 200 |
| GLN | 1350 | 150 | 1500 | 150 |
| TBN | 1403.25 | 145.5 | 1498 | 44 |
| CPD | 1600 | 200 | 1800 | 200 |
| KRW | 2370 | 250 | 2620 | 250 |
| KRK | 2025 | 250 | 2275 | 250 |
| RDK | 1302.7 | 112 | 1414.7 | 112 |
| TNG | 1075 | 150 | 1225 | 150 |

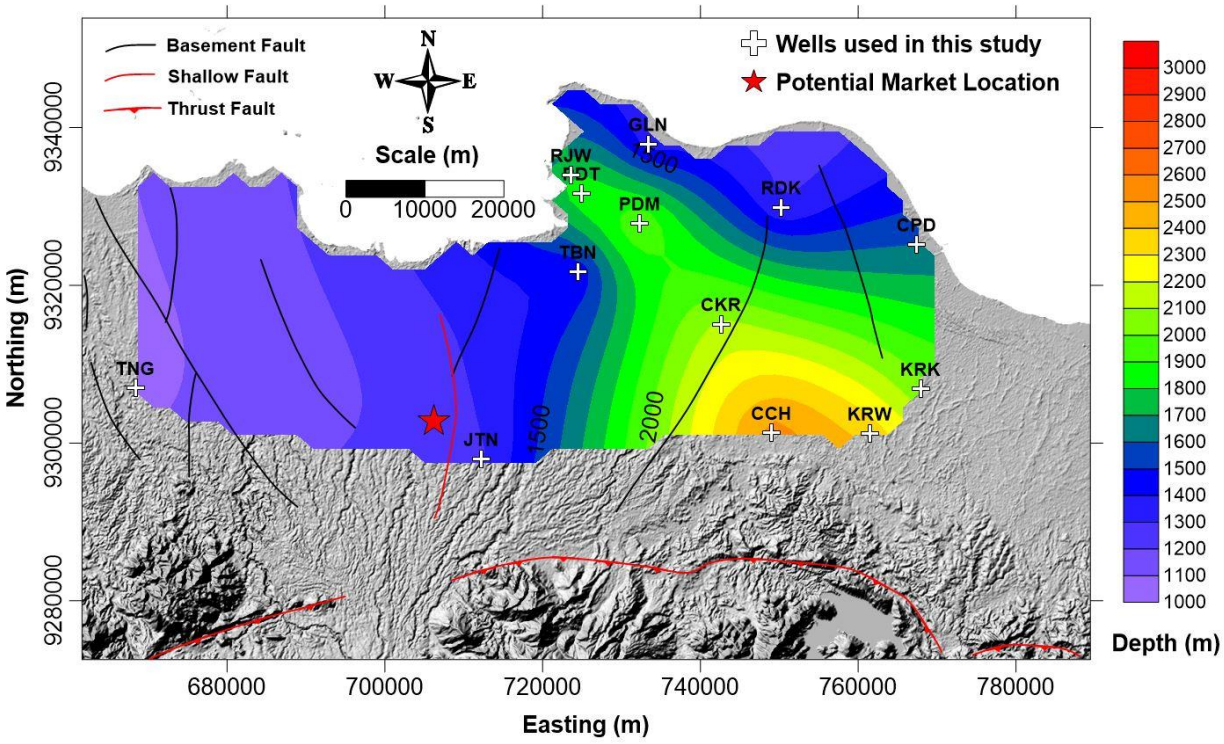


Figure 42 Map showing the distribution of depth to the center of Baturaja aquifer.

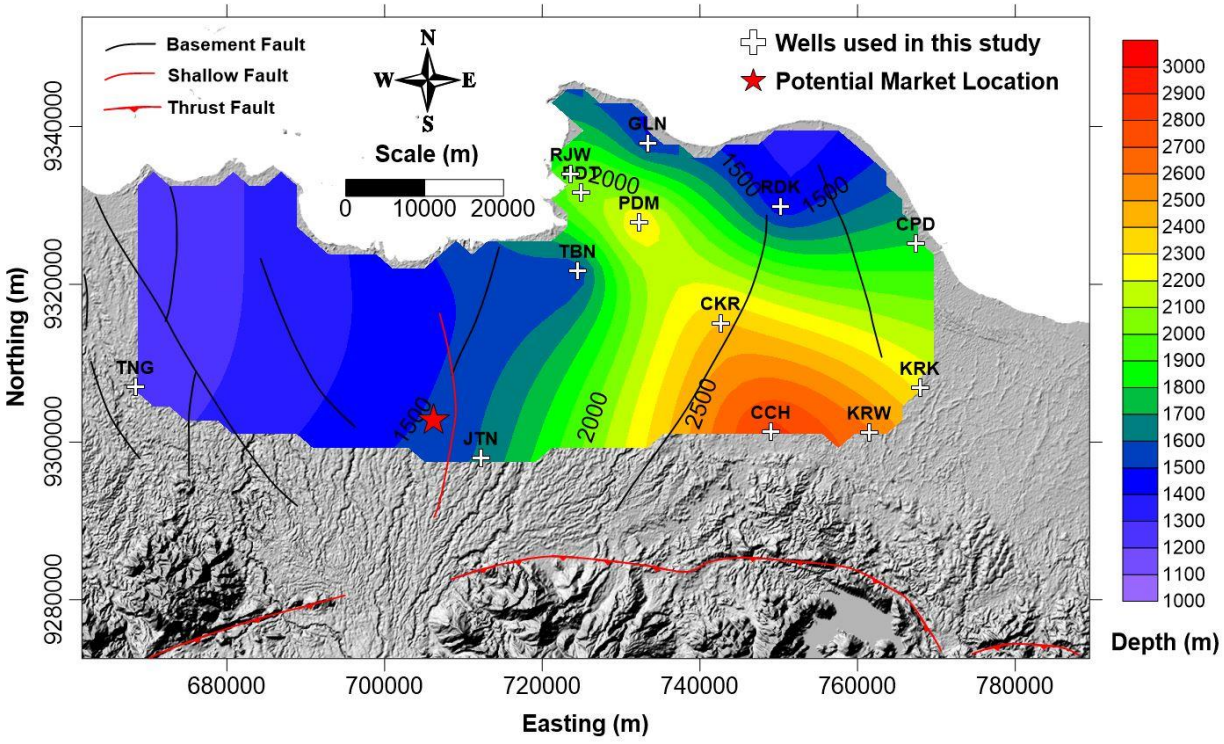


Figure 43 Map showing the distribution of depth to the center of Talang Akar aquifer.

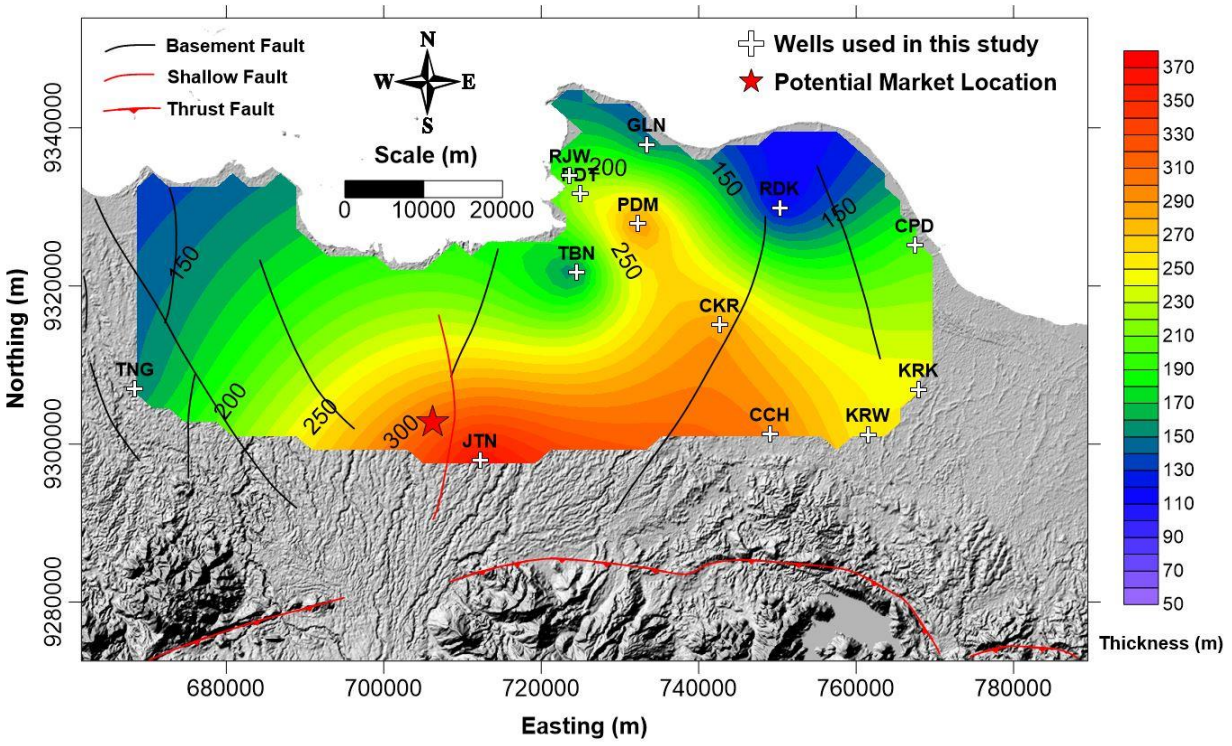


Figure 44 Map showing the distribution of thickness of the Baturaja aquifer.

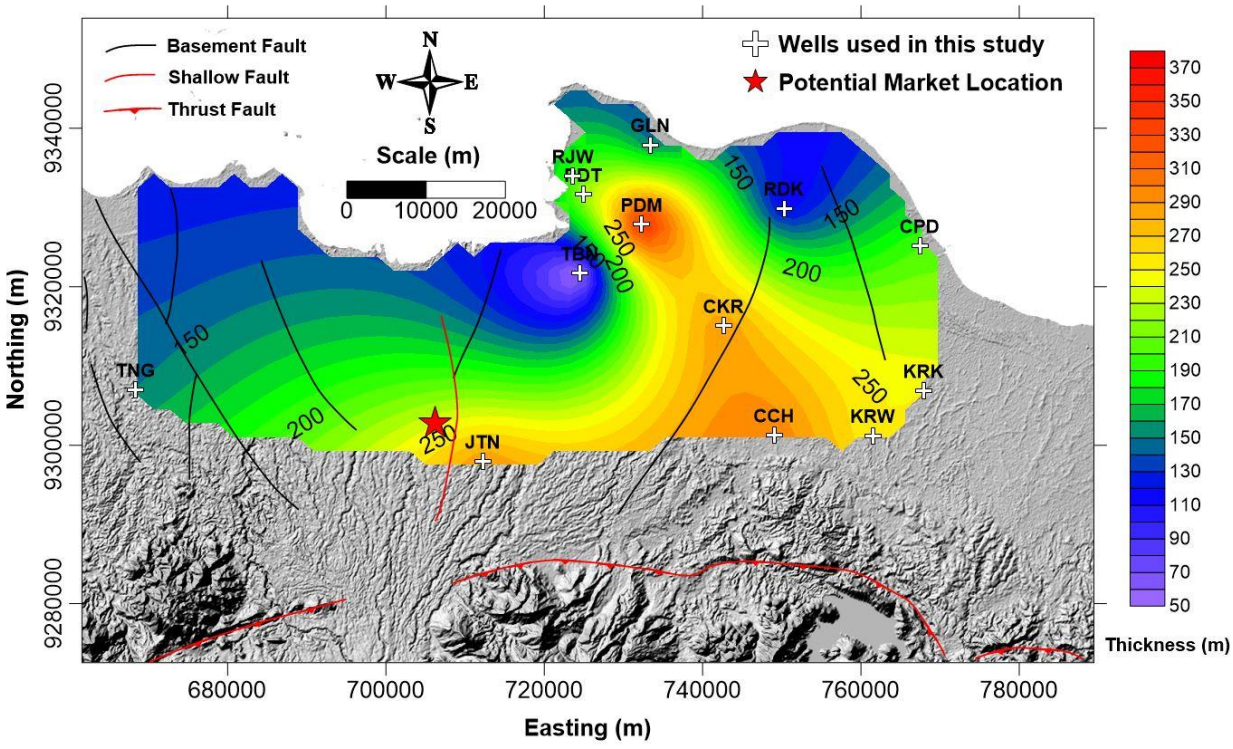


Figure 45 Map showing the distribution of thickness of the Talang Akar aquifer.

## Aquifer Temperature

The temperatures-at-depth at different locations has been mapped earlier in Part I. The temperature maps, however, are constrained to specific depths (one for each 500-meter

depth). Thus, in this part we recalculated the temperatures at the center of Baturaja and Talang Akar aquifers at different locations. For locations at which the temperature gradient value (i.e. that obtained from PT LAPI ITB, 2014) at the particular depth interval of the formation does not exist, we use the modelled temperature of Putra (2015). The calculated temperatures are listed in **Table 3**, while the aquifer temperature maps are given in **Figure 46 and 47**.

Table 3 Tabulated temperature within the Baturaja and Talang Akar aquifers. Black-colored values denote those calculated using thermal gradients derived from temperatures collated in PT LAPI ITB (2014). Blue-colored values indicate those taken from the modeled temperature of Putra (2015).

| Well | Temperature (°C) | |
|---|---|---|
| | Baturaja | Talang Akar |
| CCH | 152.61 | 168.29 |
| JTN | 96.93 | 108.49 |
| CKR | 91.9 | 117.2 |
| PDM | 110.19 | 119.2 |
| PDT | 94.12 | 102.61 |
| RJW | 117.6 | 125.63 |
| GLN | 62.69 | 68.13 |
| TBN | 59.98 | 64.71 |
| CPD | 92.8 | 106.9 |
| KRW | 85.11 | 95.74 |
| KRK | 90.23 | 100.54 |
| RDK | 61.7 | 65.45 |
| TNG | 46.51 | 49.1 |

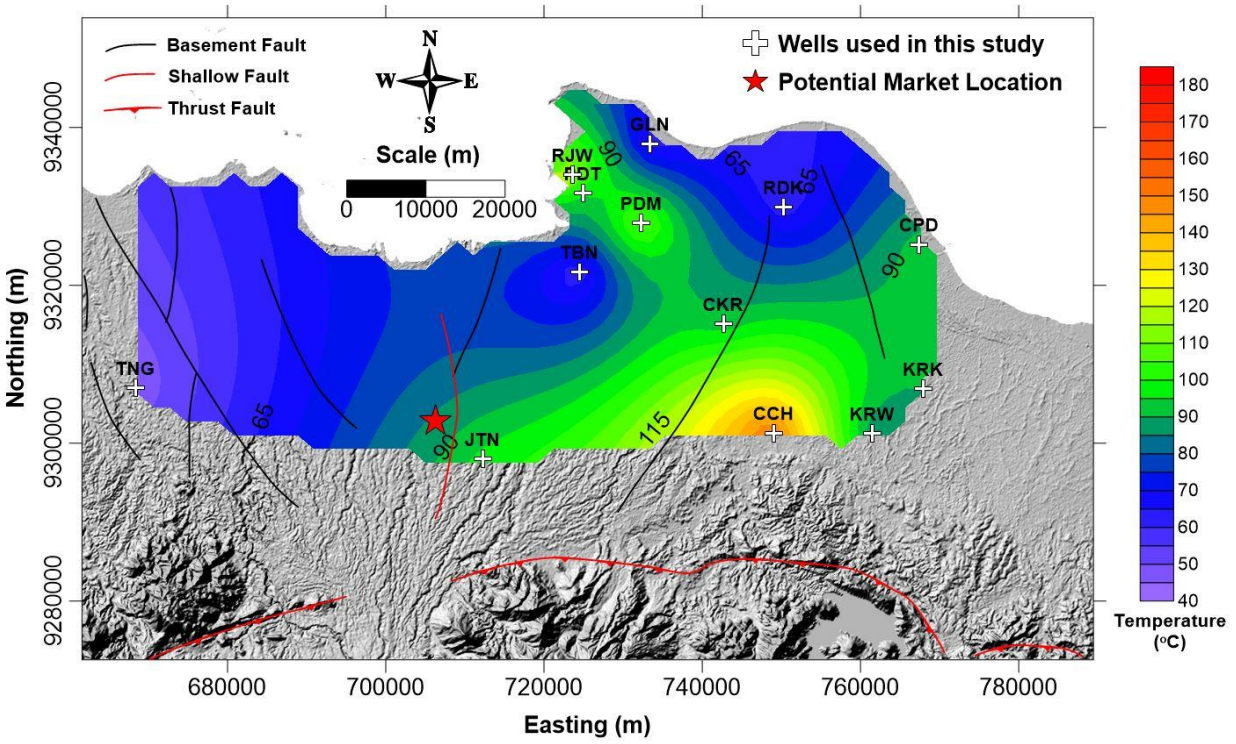


Figure 46 Map showing the distribution of temperatures within the Baturaja aquifer.

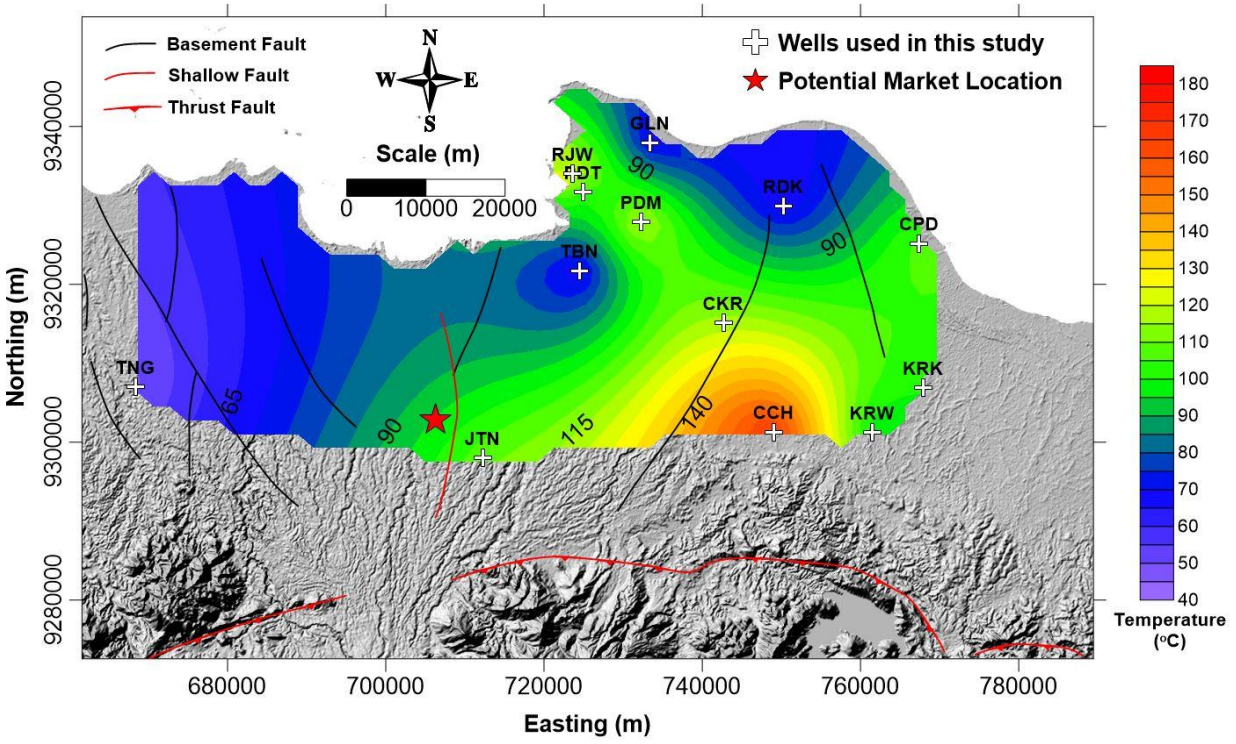


Figure 47 Map showing the distribution of temperatures within the Talang Akar aquifer.

## Aquifer Porosity

The aquifer porosities are obtained from the literature. Ideally, the determination of porosity-depth profile in wells should involve the examination of porosity logs (e.g. Sonic or Neutron

Porosity and Density Logs; Asquith and Gibson, 1982). In this case, however, by considering that the purpose of our study is to do a quick-scanning of the hot sedimentary aquifer potential within the basin, we deem that literature-derived values are just as appropriate. This is further justified by keeping in mind that in the absence of direct core measurements, even log-derived porosity values will remain subject to uncertainties. Nevertheless, we do believe that mechanical compaction, the effect of which tends to reduce porosity as burial depth increases (Allen and Allen, 2005), and the rate of which varies over different types of lithology (Beardsmore and Cull, 2001) is worth special attention. To this end, we utilize three different compaction models: Sclater and Christie (1980)'s exponential model, Falvey and Middleton (1981)'s reciprocal model, and Baldwin and Butler (1985)'s power-law model. The surface porosity values are obtained from Hantschel and Kauerauf (2009). For the Baturaja aquifer, the depositional (surface or original) porosity is taken to be 0.35 (Appendix A of Hantschel and Kauerauf, 2009) close to the reported value of 0.34 (PT LAPI ITB, 2014), while for the Talang Akar aquifer it is 0.40, representing clay-rich sandstone's (Appendix A of Hantschel and Kauerauf, 2009). The resulting three different porosity values are subsequently averaged. The averaged porosity values for each well and each aquifer is listed in **Table 4**, while the maps are given in **Figure 48** and **49**.

Table 4 Calculated porosity values of the Baturaja and Talang Akar aquifers. Each model number refers to different compaction models. 1: Sclater and Christie (1980) exponential model, 2: Falvey and Middleton (1981) reciprocal model, and 3: Baldwin and Butler (1985) power-law model.

| Well | Porosity Fraction (Batu Raja) | | | Porosity Fraction (Talang Akar) | | |
|---|---|---|---|---|---|---|
| | Model 1 | Model 2 | Model 3 | Model 1 | Model 2 | Model 3 |
| CCH | 0.18 | 0.21 | 0.15 | 0.19 | 0.21 | 0.14 |
| JTN | 0.25 | 0.26 | 0.23 | 0.26 | 0.27 | 0.2 |
| CKR | 0.2 | 0.22 | 0.17 | 0.21 | 0.23 | 0.16 |
| PDM | 0.2 | 0.23 | 0.18 | 0.21 | 0.23 | 0.16 |
| PDT | 0.21 | 0.23 | 0.19 | 0.23 | 0.24 | 0.17 |
| RJW | 0.22 | 0.23 | 0.19 | 0.23 | 0.25 | 0.18 |
| GLN | 0.24 | 0.26 | 0.22 | 0.27 | 0.27 | 0.21 |
| TBN | 0.24 | 0.25 | 0.22 | 0.27 | 0.27 | 0.21 |
| CPD | 0.23 | 0.24 | 0.21 | 0.25 | 0.26 | 0.19 |
| KRW | 0.18 | 0.21 | 0.16 | 0.2 | 0.22 | 0.15 |
| KRK | 0.20 | 0.23 | 0.18 | 0.22 | 0.23 | 0.16 |
| RDK | 0.25 | 0.26 | 0.23 | 0.27 | 0.28 | 0.22 |
| TNG | 0.26 | 0.27 | 0.25 | 0.29 | 0.29 | 0.24 |

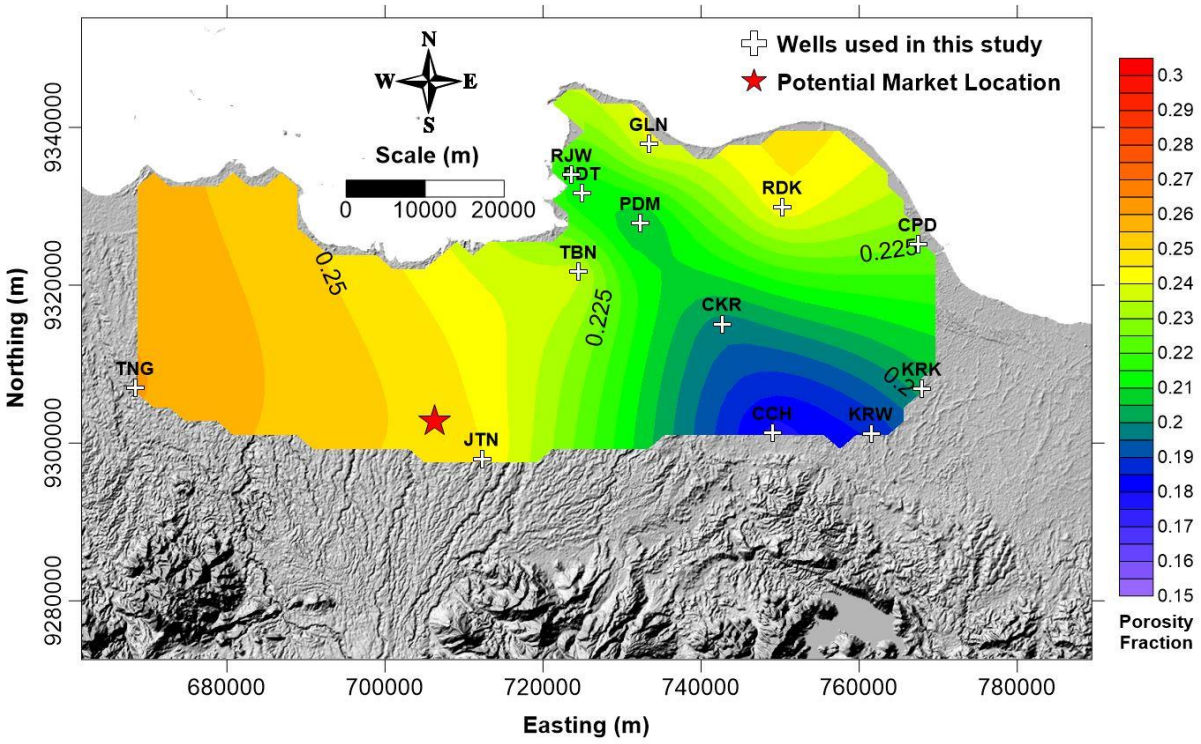


Figure 48 Map showing the distribution of average porosity values within the Baturaja aquifer.

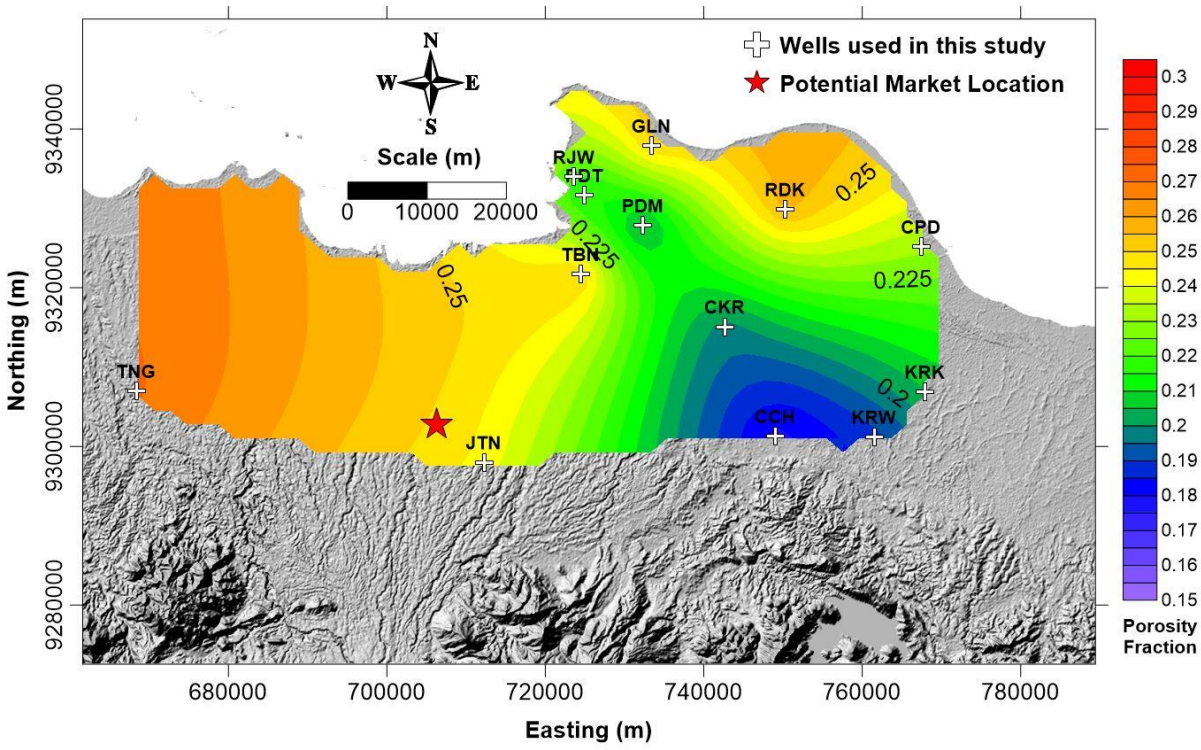


Figure 49 Map showing the distribution of average porosity values within the Talang Akar aquifer.

## Aquifer Permeability and Transmissivity

Information on aquifer permeability values is obtained from PT LAPI ITB (2014). Note that permeability as addressed in this study refers to primary (matrix) permeability. Information regarding fracture permeability is absent, though their positions may be roughly estimated from near-surface or basement faults' (see **Figure 35** of Part Regional). Since there are many wells for which permeability value was not reported due to it being absent in the well report, we resorted to using literature values, like porosity. In order to create more "realistic" values, we estimate the permeability-at-depth of sandstone and shale of the Talang Akar aquifer by relating it to the calculated porosities using the well-known Kozeny-Carman relationship (Hantschel and Kauerauf, 2009). Because the permeability of sandstone and shale must be computed separately when using the relationship, the permeability of Talang Akar formation at a location is assumed to be the average between the calculated values of the two lithologies. In contrast, following a similar approach to Allis and Kirby (2013), we directly obtain permeability values from the average carbonate permeability-porosity values contained in the **Table 1** of Ehrenberg and Nadeau (2005) for the limestone of Baturaja aquifer. As previously explained, there are different porosity values derived from the three compaction models, thus we use the average of the three values to assign and compare with the porosity-permeability relationship data of Ehrenberg and Nadeau (2005). The transmissivity values are then found by multiplying permeability by the aquifer thicknesses at each well. The permeability and transmissivity values (the intermediate values) are given in **Table 5**, and the maps of these parameters are shown in **Figure 50** to **53**.

Table 5 Calculated permeability and transmissivity values of the Baturaja and Talang Akar aquifers.

| Well | Batu Raja | | Talang Akar | |
|---|---|---|---|---|
| | Permeability (mD) | Transmissivity (D.m) | Permeability (mD) | Transmissivity (D.m) |
| CCH | 58 | 17.4 | 9.53 | 2.86 |
| JTN | 100 | 37.1 | 31.43 | 9.18 |
| CKR | 58 | 16.8 | 14.39 | 4.16 |
| PDM | 58 | 17.3 | 15.48 | 5.53 |
| PDT | 58 | 13.7 | 19.43 | 4.33 |
| RJW | 58 | 11.6 | 21.43 | 4.29 |
| GLN | 100 | 15.0 | 35.17 | 5.28 |
| TBN | 100 | 14.6 | 35.24 | 1.55 |
| CPD | 100 | 20.0 | 26.08 | 5.22 |
| KRW | 58 | 14.5 | 11.83 | 2.96 |
| KRK | 58 | 14.5 | 16.42 | 4.11 |
| RDK | 100 | 11.2 | 38.34 | 4.29 |

| Well | Batu Raja | | Talang Akar | |
|---|---|---|---|---|
| | Permeability (mD) | Transmissivity (D.m) | Permeability (mD) | Transmissivity (D.m) |
| TNG | 100 | 15.0 | 46.53 | 6.98 |

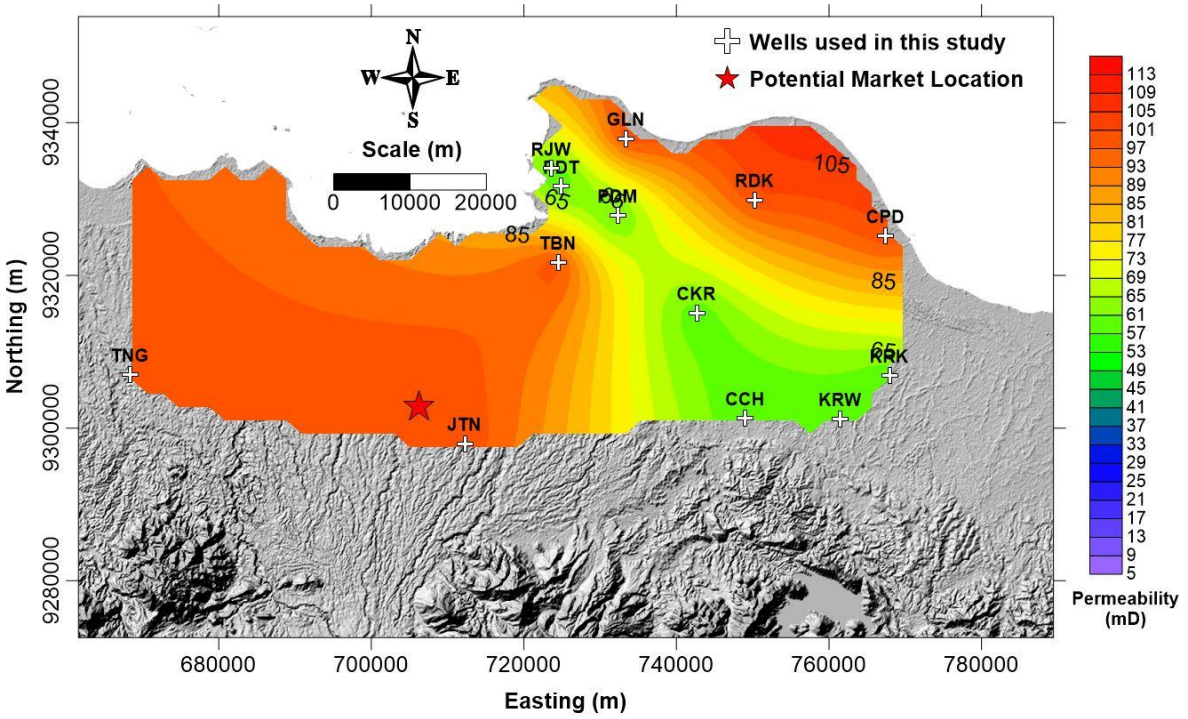


Figure 50 Map showing the distribution of permeability values within the Baturaja aquifer.

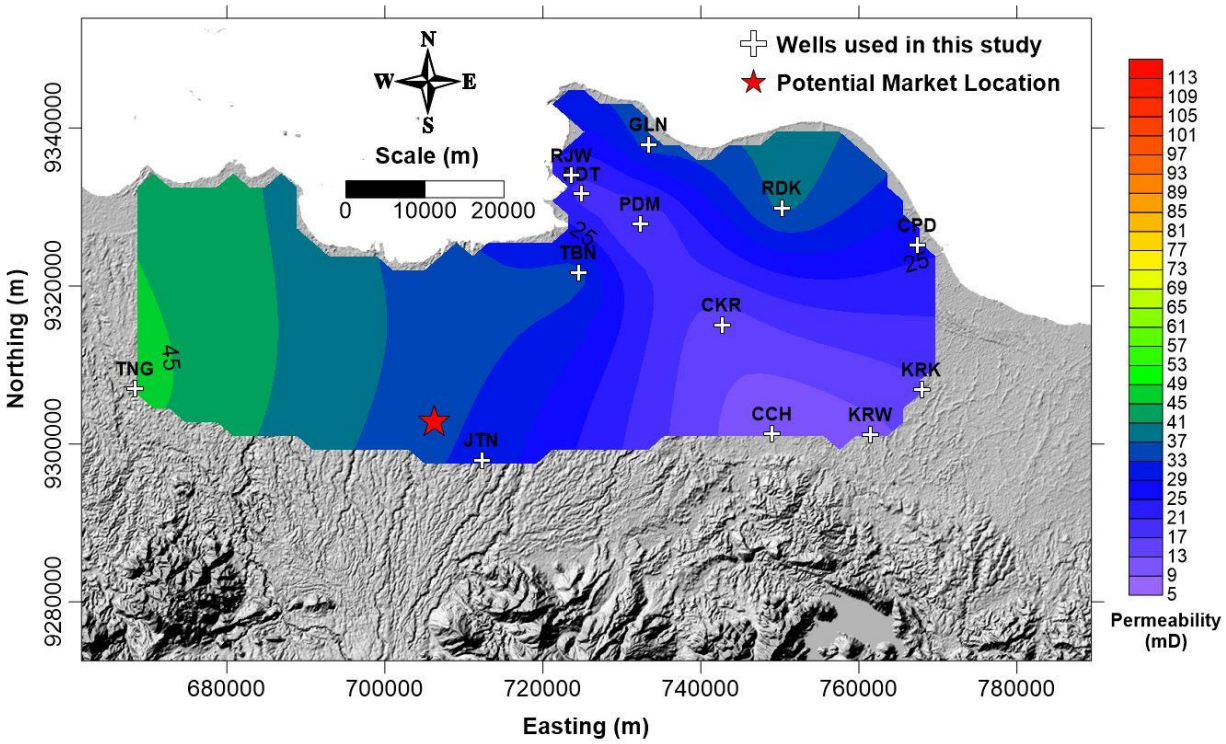


Figure 51 Map showing the distribution of permeability values within the Talang Akar aquifer.

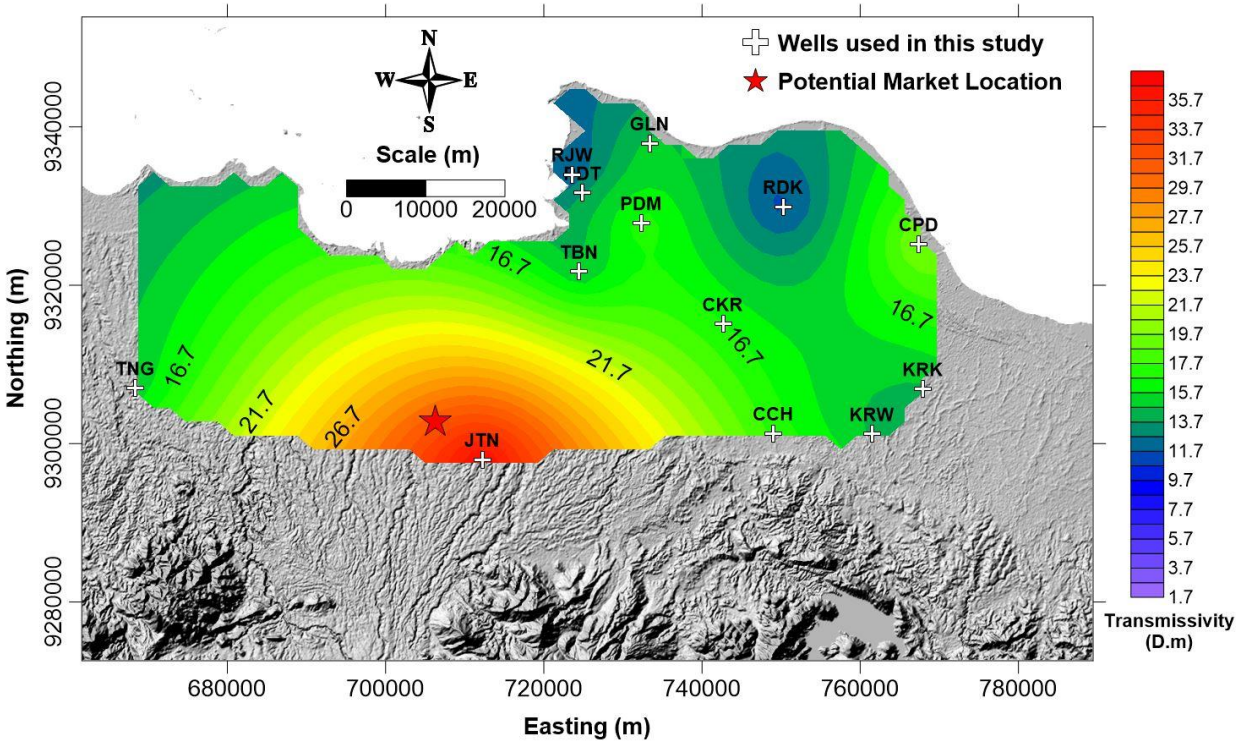


Figure 52 Map showing the distribution of transmissivity values within the Baturaja aquifer.

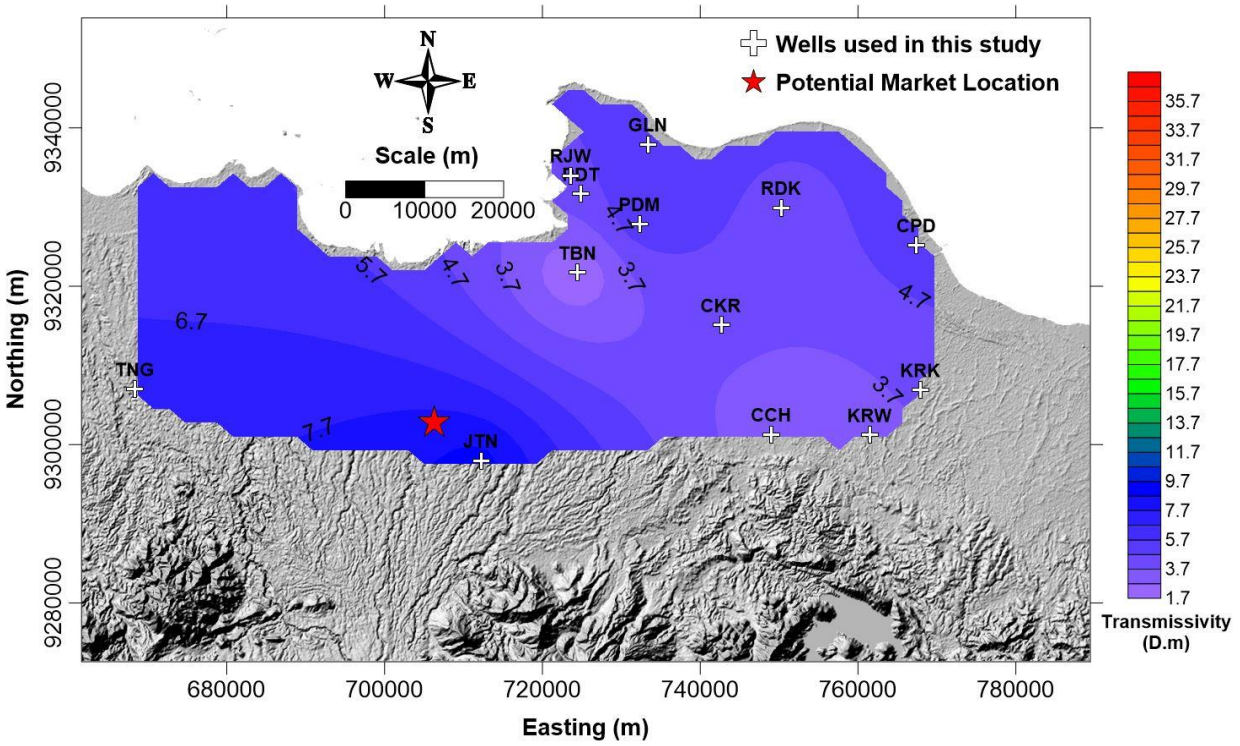


Figure 53 Map showing the distribution of transmissivity values within the Talang Akar aquifer.

## Uncertainty Analysis

A Monte Carlo analysis was performed to assess the impact uncertainties in reservoir parameter values on the estimate of resource potential. The uncertainties in reservoir parameters, i.e. thickness, depth, temperature, and porosity, are obtained from the standard deviations of their means, which in turn are derived from the average values of all wells. The reservoir parameter values used in the Monte Carlo analysis are listed in **Table 6**. The mean value of each parameter was adopted as the most likely, while the minimum and maximum values are adopted from the minimum and maximum values of each parameter for the two aquifers listed in **Tables 2** to **4**.

Table 6 Reservoir parameters used in Monte Carlo analysis.

| Aquifer Parameter | Baturaja | | | Talang Akar | | |
|---|---|---|---|---|---|---|
| | Minimum | Most Likely | Maximum | Minimum | Most Likely | Maximum |
| Thickness (m) | 112 | 227.12 | 371 | 44 | 216.69 | 357 |
| Temperature (°C) | 46.51 | 89.41 | 152.61 | 49.10 | 99.38 | 168.29 |
| Porosity | 0.18 | 0.22 | 0.26 | 0.18 | 0.22 | 0.27 |

In addition to the reservoir parameters, several other reservoir and geothermal power production-related parameters are also introduced to the Monte Carlo calculation. First, the reservoir area is maintained at a single value of 3392.478 $km^2$, assuming that all parts of the aquifers within the studied area's boundary are water-saturated (the temperature may differ). The rock density value was arbitrarily assumed to be 2500, 2600, 2700 $kg/m^3$ and the rock heat capacity is set at 1 kJ/kg.°C, the average value of most rocks (Blackwell et al., 2007). The final temperature, i.e. when the temperature of the extraction well is that of reinjection temperature (e.g. due to thermal breakthrough), is assumed to be similar to that of surface temperature (28 °C), because at this condition the geothermal heat energy from the aquifers may still be used for direct spatial heating-cooling (e.g. Kramers et al., 2012). Reservoir life time and recovery factor are taken to be 30 years (e.g. Kramers et al., 2012) and 33% of the aquifer maximum heat content (van Wees et al., 2012), respectively. In reality, these parameters may vary greatly according the actual subsurface conditions, e.g. whether or not an advective background flow is present for a geothermal doublet (Wellmann et al., 2010), and/or if the proposed extraction scheme uses a certain set of well doublet pattern, number, and spacing (Gringarten, 1978). In fact, as explained in the methodology, the aquifer thickness itself may influence the behavior of the reservoir (Poulsen et al, 2015). The additional parameters are tabulated in **Table 7**. Due to the limitation of the default program, which was developed in Macro Excel, the computed resource potential values are directly given in the form of technical potential, instead of stored heat. We can find the original stored heat magnitudes by multiplying these values by the lifetime and dividing them by the

recovery factors used as inputs to the Monte Carlo simulation. The final estimated geothermal resource potential of the Baturaja and Talang Akar aquifers along with its uncertainty are displayed in **Table 8**.

Table 7 Other parameters used in Monte Carlo analysis.

| Parameter | Baturaja | | | Talang Akar | | |
|---|---|---|---|---|---|---|
| | Minimum | Most Likely | Maximum | Minimum | Most Likely | Maximum |
| Area ($km^2$) | 3392.478 | | | | | |
| Rock Heat Capacity (kJ/kg.$^oC$) | 1 | | | | | |
| Rock Density ($kg/m^3$) | 2500 | 2600 | 2700 | 2500 | 2600 | 2700 |
| Final Temperature ($^oC$) | 28 | | | | | |
| Recovery Factor | 0.33 | | | | | |
| Reservoir Lifetime (years) | 30 | | | | | |
| Initial Water Saturation | 1 | | | | | |
| Final Water Saturation | 1 | | | | | |
| Random Numbers | 20000 | | | | | |

Table 8 Results of Monte Carlo analysis.

| Parameter | Baturaja | | | Talang Akar | | |
|---|---|---|---|---|---|---|
| | Minimum | Median | Maximum | Minimum | Median | Maximum |
| Technical Potential (MWth) | 24345.14 | 48143.5 | 80813.23 | 19949.16 | 47144.61 | 84014.46 |
| Recoverable Heat (J) | $2.3 \times 10^{19}$ | $4.55 \times 10^{19}$ | $7.65 \times 10^{19}$ | $1.89 \times 10^{19}$ | $4.46 \times 10^{19}$ | $7.95 \times 10^{19}$ |
| Original Stored Heat (J) | $6.98 \times 10^{19}$ | $1.38 \times 10^{20}$ | $2.32 \times 10^{20}$ | $5.72 \times 10^{19}$ | $1.35 \times 10^{20}$ | $2.41 \times 10^{20}$ |

The above Monte Carlo analysis may involve parameters that display very large ranges between their minimum, intermediate, and maximum values. This situation may have resulted from the variation of depth to the center of aquifers which induces the variation in temperature and porosity, both of which are strong functions of depth. As a result, the calculated amount of stored Heat-in-Places (HIP) varies greatly between their minima and maxima. In order to gain more confidence in the estimated stored HIPs of both aquifers, HIP

maps were also constructed based on their temperatures, thicknesses, and porosities at each location. The estimated stored HIP maps are presented in **Figures 54** and **55**.

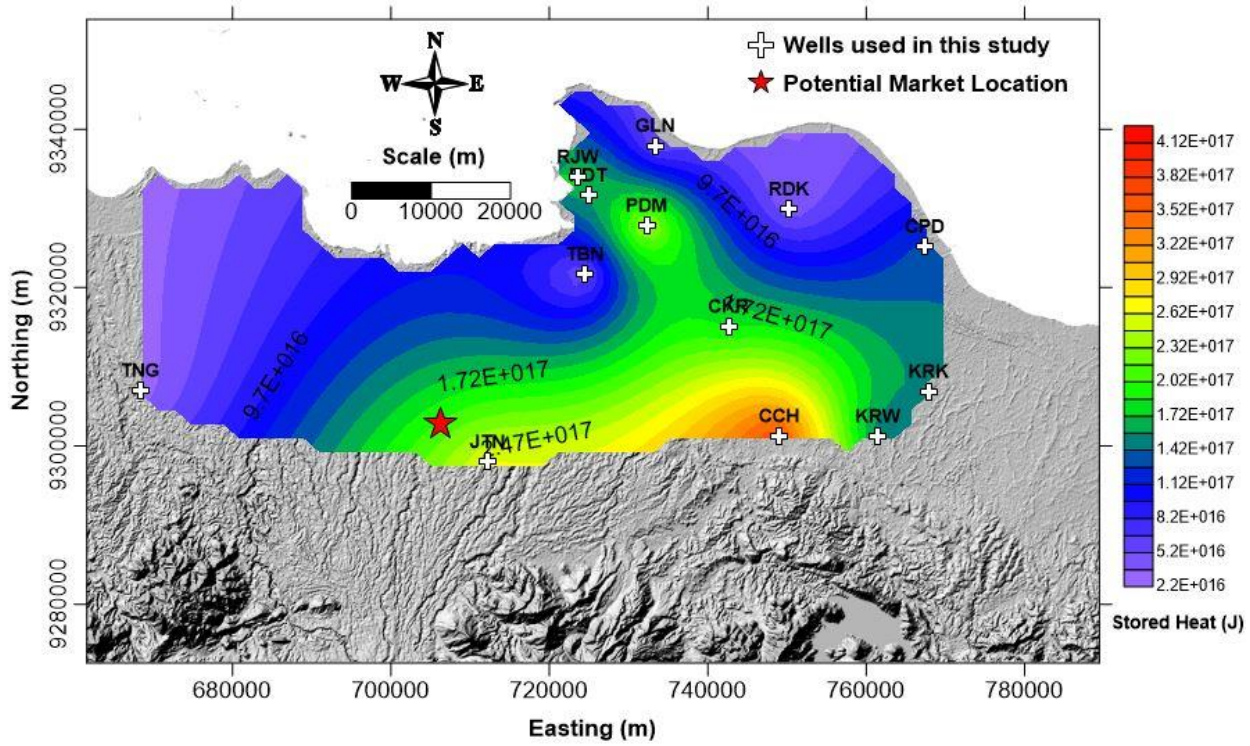


Figure 54 Map showing the distribution of estimated stored Heat-in-Place (HIP) of the Baturaja aquifer.

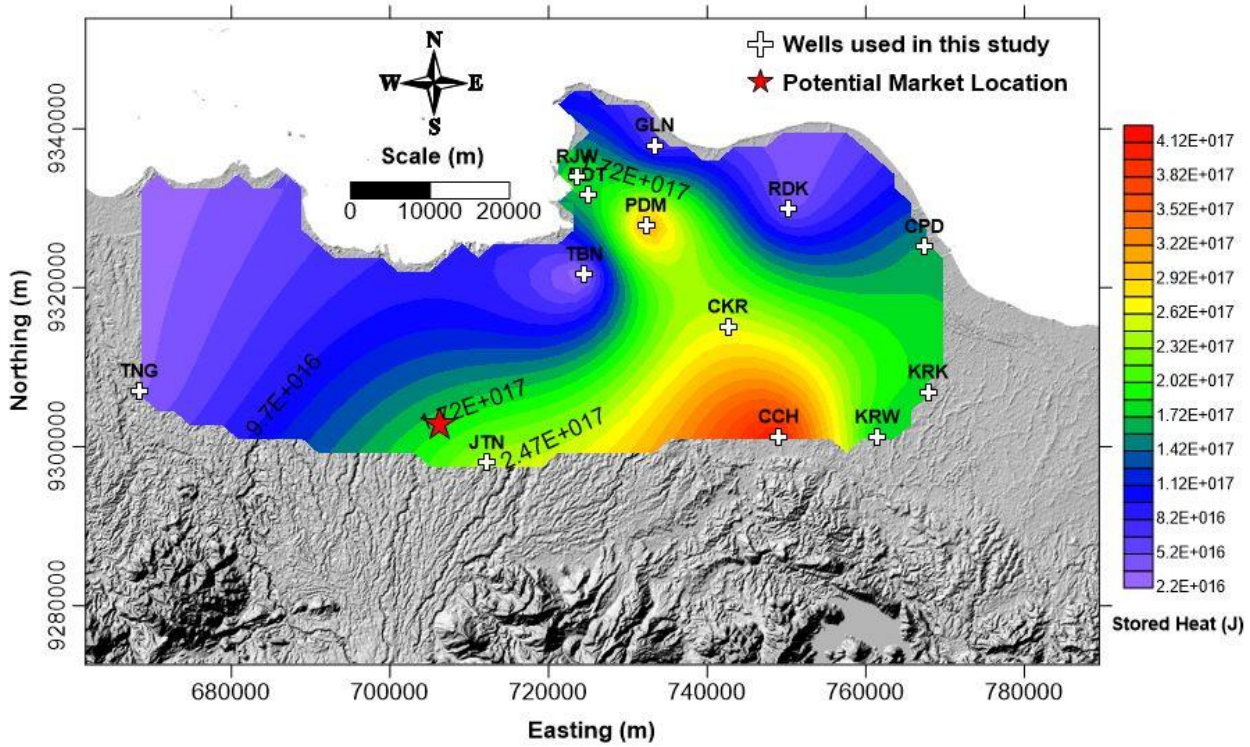


Figure 55 Map showing the distribution of estimated stored Heat-in-Place (HIP) of the Talang Akar aquifer.

Since Kriging was used in the interpolation process, these maps allow for the visualization of spatial uncertainty of the calculated HIP at each location for each prospective aquifer. However, since the differences in both magnitudes and spatial pattern between the Baturaja and Talang Akar aquifers that can be observed from **Figures 54** and **55** are not significant, their Kriging-derived spatial uncertainties are pretty much similar, so that only one map of which is presented (**Fig. 56**).

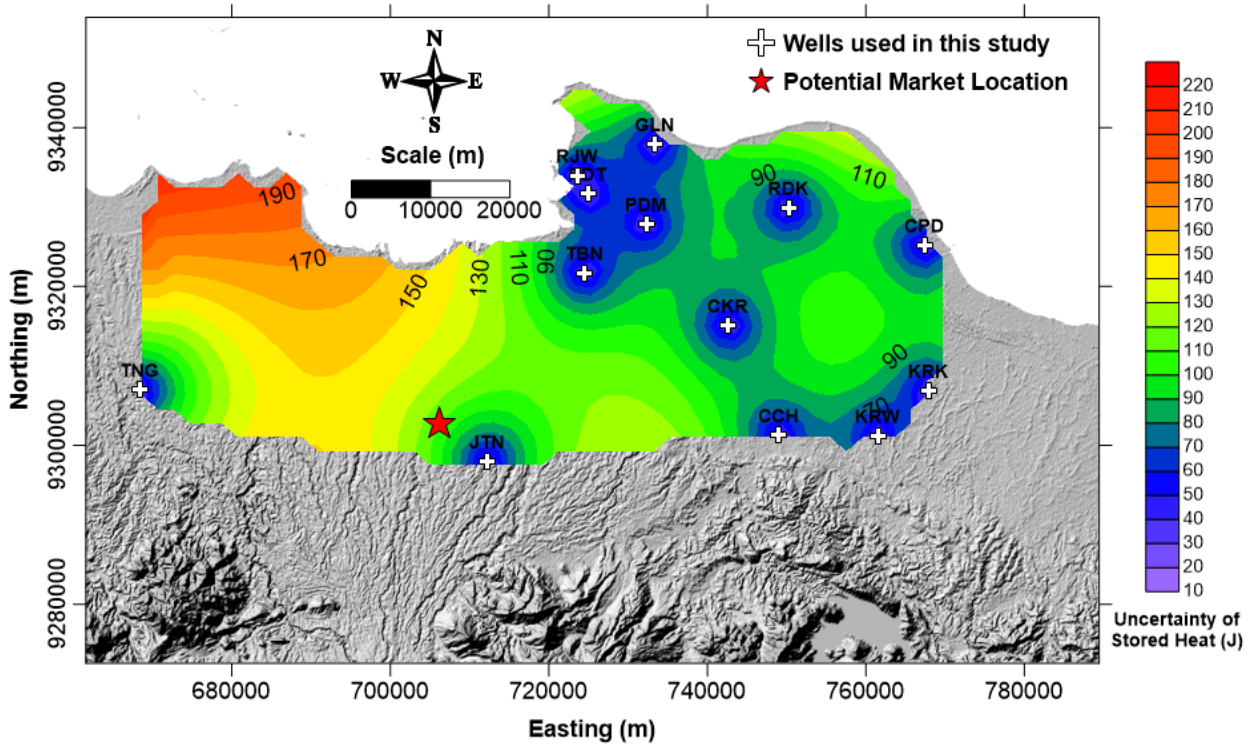


Figure 56 Map showing the distribution Kriging-derived spatial uncertainty of the estimated stored Heat-in-Place (HIP) of Baturaja and Talang Akar aquifers.

## Calculation of Flow Rate and Thermal Power

In addition to the stored heat values, the flow rate and thermal power of each well were calculated and presented in **Table 9**. A map was also constructed for the latter (**Figure 57** and **58**) and their uncertainty derived from the Kriging interpolation (**Figure 59**). The Kriging-derived uncertainty possesses a similar range to that of stored heat, probably due to the default variogram model used by Surfer, that is, a linear variogram with a slope of 1.0.

Table 9 Calculated flow rate and thermal power of the Baturaja and Talang Akar aquifers.

| Well | Batu Raja | | Talang Akar | |
|---|---|---|---|---|
| | Flow Rate ($m^3/h$) | Thermal Power (MW) | Flow Rate ($m^3/h$) | Thermal Power (MW) |
| CCH | 578.8 | 79.14 | 651.7 | 100.32 |

| | | | | |
|---|---|---|---|---|
| JTN | 320.2 | 24.22 | 373.9 | 33.02 |
| CKR | 296.8 | 20.81 | 414.4 | 40.56 |
| PDM | 381.8 | 34.43 | 423.6 | 42.39 |
| PDT | 307.2 | 22.29 | 346.6 | 28.37 |
| RJW | 416.2 | 40.92 | 453.5 | 48.58 |
| GLN | 161.1 | 6.13 | 186.4 | 8.21 |
| TBN | 148.6 | 5.21 | 170.5 | 6.87 |
| CPD | 301.0 | 21.40 | 366.5 | 31.73 |
| KRW | 265.3 | 16.62 | 314.7 | 23.39 |
| KRK | 289.1 | 19.74 | 337.0 | 26.82 |
| RDK | 156.5 | 5.79 | 174.0 | 7.15 |
| TNG | 86.0 | 1.75 | 98.0 | 2.27 |

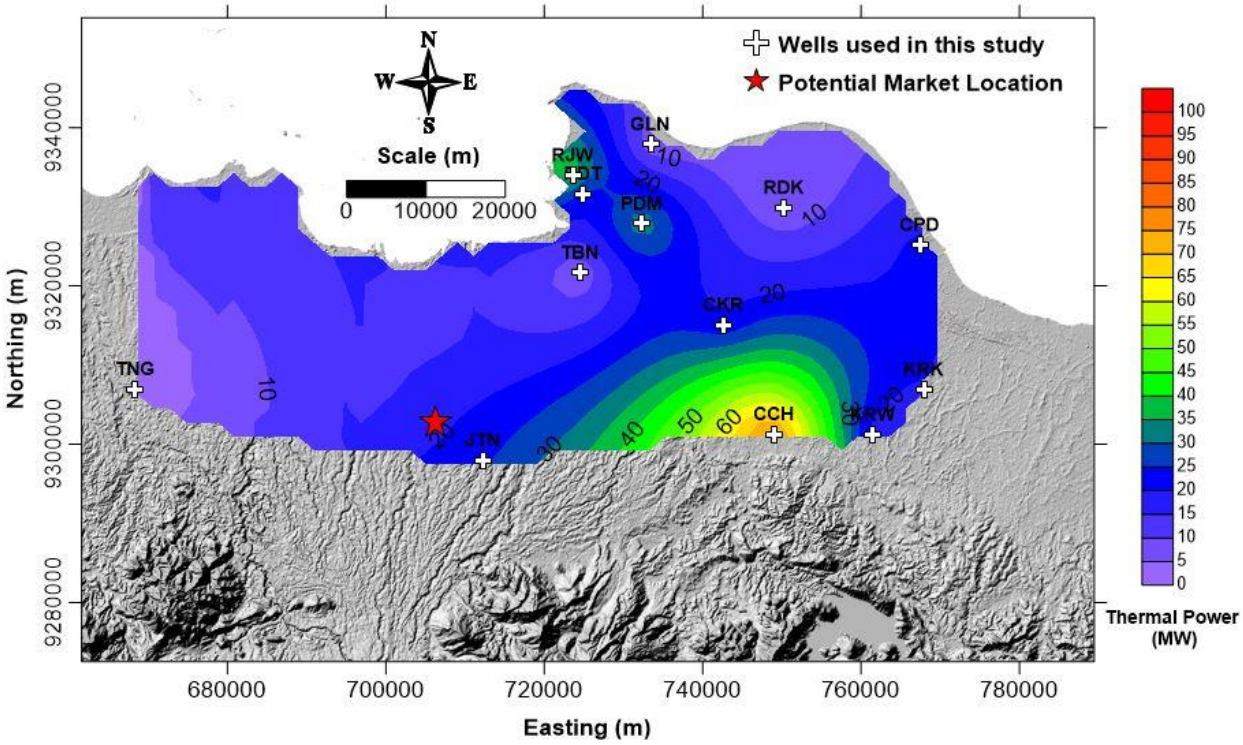


Figure 57 Map showing the distribution of calculated well thermal power of the Baturaja aquifer.

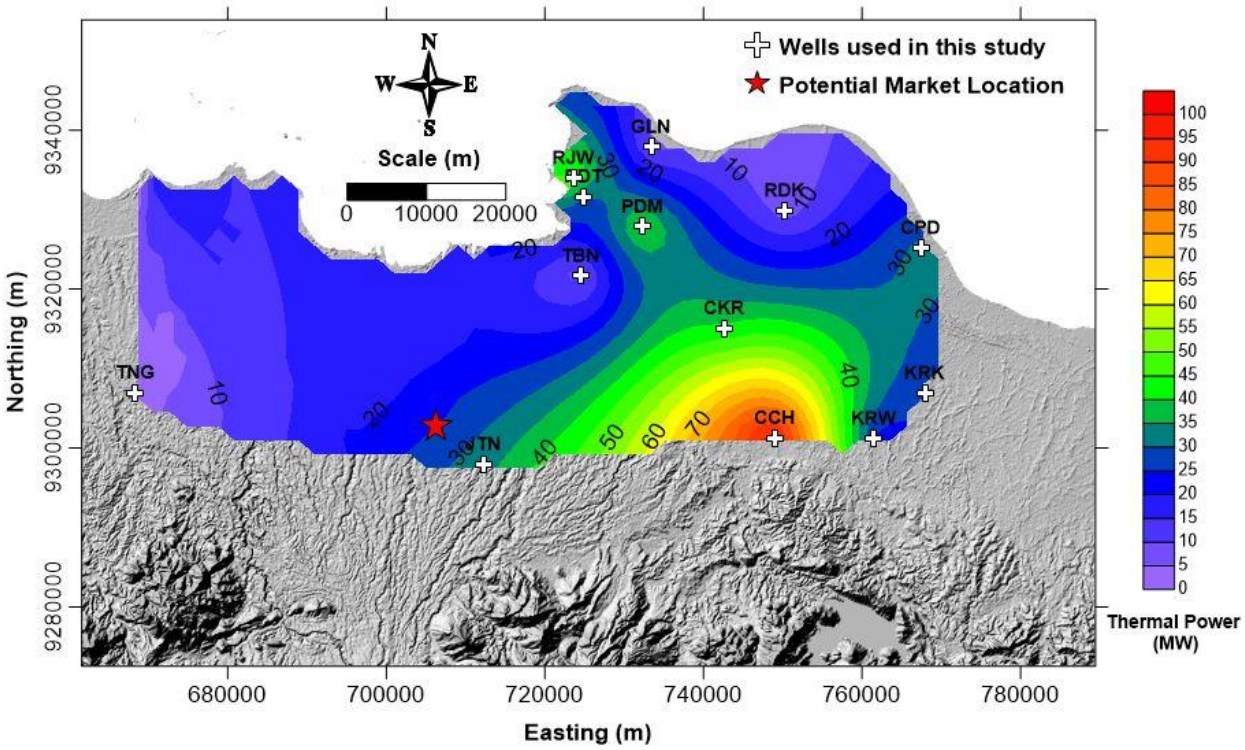


Figure 58 Map showing the distribution of calculated well thermal power of the Talang Akar aquifer.

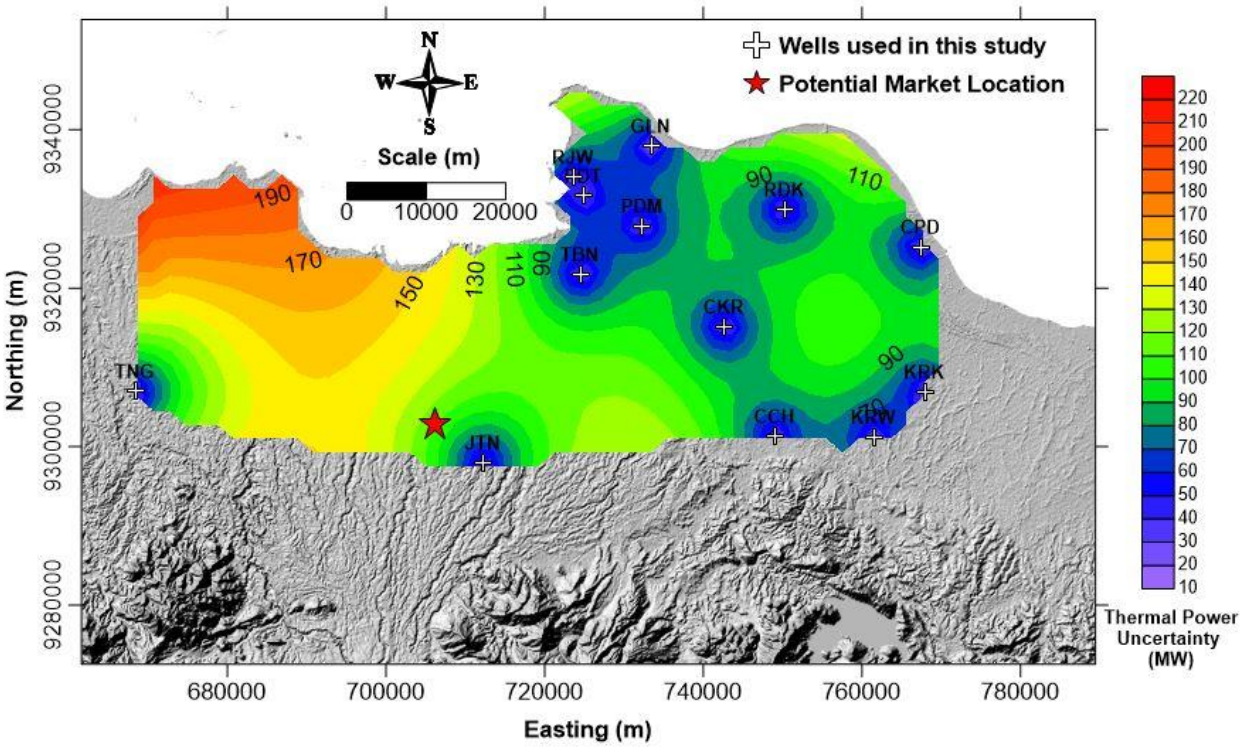


Figure 59 Map showing the distribution Kriging-derived spatial uncertainty of the calculated well thermal power of Baturaja and Talang Akar aquifers.

## 2.3 WASTE HEAT FROM GEOTHERMAL POWER PLANT

| TYPE OF RESOURCE | NO | REGENCY/ KABUPATEN | GEOTHERMAL PROSPECT | COMPANY | TYPE OF FLUID | INSTALLED CAPACITY (MW) | | POWER PLANT CYCLE | P SEPARATOR (bara) | | P TURBINE (bara) | | P CONDENSOR (bara) | |
|---|---|---|---|---|---|---|---|---|---|---|---|---|---|---|
| WASTE HEAT | 1 | BANDUNG | Kamojang | PERTAMINA GEOTHERMAL ENERGY AREA KAMOJANG | Vapor dominated | UNIT I | 30 | Direct Dry Steam-Single Flash | UNIT I | 10 | UNIT I | 6.5 | UNIT I | 0.133 |
| | | | | | | UNIT II | 55 | | UNIT II | 10 | UNIT II | 6.5 | UNIT II | 0.1 |
| | | | | | | UNIT III | 55 | | UNIT III | 10 | UNIT III | 6.5 | UNIT III | 0.1 |
| | | | | | | UNIT VI | 60 | | UNIT VI | 11.3 | UNIT VI | 11 | UNIT VI | 0.14 |
| | 2 | | Wayang Windu | STAR ENERGY WAYANG WINDU | Two phase-vapor dominated | UNIT I | 110 | Separated Steam-Single Flash | UNIT I | 10.43 | UNIT I | 10.2 | UNIT I | 0.12 |
| | | | | | | UNIT II | 117 | | UNIT II | 10.45 | UNIT II | 10.7 | UNIT II | 0.12 |
| | 3 | | Patuha | GEO DIPA ENERGI | Two phase-vapor dominated | UNIT I | 60 | Separated Steam-Single Flash | UNIT I | 7 (Demister) | UNIT I | 7 | UNIT I | 0.1 |
| | 4 | BOGOR | Awibengkok-G. Salak | CHEVRON GEOTHERMAL SALAK | Liquid dominated | UNIT I | 60 | Separated Steam-Single Flash | UNIT I | - | UNIT I | 6.2 | UNIT I | 0.09 |
| | | | | | | UNIT II | 60 | | UNIT II | - | UNIT II | 6.2 | UNIT II | |
| | | | | | | UNIT III | 60 | | UNIT III | - | UNIT III | 6.2 | UNIT III | |
| | | | | | | UNIT IV | 65.6 | | UNIT IV | - | UNIT IV | 6.9 | UNIT IV | 0.1 |
| | | | | | | UNIT V | 65.6 | | UNIT V | - | UNIT V | 6.9 | UNIT V | |
| | | | | | | UNIT VI | 65.6 | | UNIT VI | - | UNIT VI | 6.9 | UNIT VI | |
| | 5 | GARUT | Darajat | CHEVRON GEOTHERMAL INDONESIA | Vapor dominated | UNIT I | 55 | Direct Dry Steam-Single Flash | UNIT I | - | UNIT I | 10 | UNIT I | 0.1 |
| | | | | | | UNIT II | 95 | | UNIT II | - | UNIT II | 13 | UNIT II | 0.1 |
| | | | | | | UNIT III | 121 | | UNIT III | - | UNIT III | 16.6 | UNIT III | 0.1 |
| | | | | | | | 1134.8 | | | | | | | |

Figure 60 Installed geothermal power plant in West Java showing type of fluid produced, power plant cycle, pressure of separator, turbine, and condensor.

| TYPE OF RESOURCE | NO | REGENCY/ KABUPATEN | GEOTHERMAL PROSPECT | COMPANY | Number of Brine Wells (No of Wellpad) | Number of Condensate Wells (No of Wellpad) | Total Flowrate of Brine Wells | Temp of Brine Wells (deg C) | Minimum Temp of Injection | Pressure of Brine Wells (bar) | Total Flowrate of Condensate Wells | Pressure of Condensate Wells (bar) |
|---|---|---|---|---|---|---|---|---|---|---|---|---|
| WASTE HEAT | 1 | BANDUNG | Kamojang | PERTAMINA GEOTHERMAL ENERGY AREA KAMOJANG | - | 4 (15; 20; 35; 55) | - | - | 40 | - | 6000 (L/m) | - |
| | 2 | | Wayang Windu | STAR ENERGY WAYANG WINDU | 1 | 3 | 50-60 kg/s | 180 | - | 5.6 | 80-100 | 5.3; -0.9; -0.7 |
| | 3 | | Patuha | GEO DIPA ENERGI | 1 | | 89-111 ton/hour | | | | | - |
| | 4 | BOGOR | Awibengkok-G. Salak | CHEVRON GEOTHERMAL SALAK | 2 (pad 14) | 7(6) | ± 2000 kph (total) kilopounds per hour or 252 kg/s | 173.4 | - | - | 6966 (ton/h) | - |
| | 5 | GARUT | Darajat | CHEVRON GEOTHERMAL INDONESIA | - | 1 | - | - | 40 | - | 135 liter/s | - |

Figure 61 Installed geothermal power plant in West Java showing data of flowrate and temperature of brine and condensate

Kamojang and Darajat are dry-steam geothermal fields, therefore there is no brine producing from the reservoir. The water reinjected into reservoir comes from condensate water which commonly has temperature around 40℃. However waste heat from steam can still be potential for direct use because the steam temperature from Kamojang and Darajat is

around 225℃, high enough to have additional use especially for direct use. For example in Kamojang, there is mushroom cultivation organized by PT Pertamina Geothermal Energy as their CSR, in which soon is expected to be run by local private enterprise in Kamojang area. In two-phase geothermal fields, for example, Wayang Windu, Awibengkok, and Patuha, beside steam, liquid or brine is also produced from reservoir. Then it is separated from steam by separator, to be reinjected into the reservoir. The temperature of brine is commonly around 140-170℃, adequate to install some technology for direct use. In addition to that, the flow rate as depicted in **Figure 61** is relatively high. Especially from Awibengkok which is two-phase geothermal field with liquid-dominated. Hence more brine can be produced from the reservoir. While Patuha and Wayang Windu are two-phase geothermal field with vapor-dominated, therefore more steam is produced. Mostly surrounding the power plant are plantation area. Almost every geothermal power plants in Indonesia are surrounded by tea plantation (**Fig. 63**), coffee plantation, and other agricultural products. Unfortunately, there is no application which has utilized waste heat from brine in West Java province geothermal power plant.

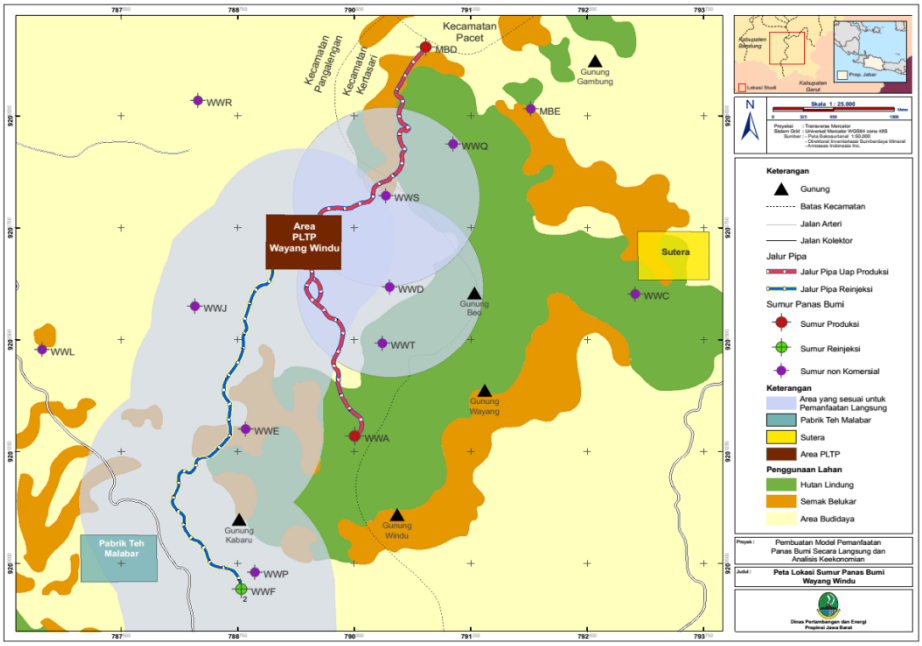


Figure 62 Map of Wayang Windu geothermal area

(Information: Area PLTP = Geothermal Power Plant Area, Area yang sesuai untuk Pemanfaatan Langsung = Recommended Area for Direct Use, Pabrik Teh Malabar = Malabar Tea Factory, Hutan Lindung = Protection Forest, Sumur Produksi = Production well, Sumur Injeksi = Injection well, Sumur non Komersial = Non commercial well)

Figure 63 Tea plantation in Wayang Windu area

**Figure 62** showing map of Wayang Windu geothermal field, where Malabar Tea Factory is located only 1.5 km from the nearest injection well.